博士論文

Ph.D. Dissertation

ロボットアームを制御するための上肢運動に基づく筋電図（EMG）信号マッピングと分析

Electromyography (EMG) signal mapping and analysis based on upper-limb motion for controlling robotic arm

Year 2021（2021 年)

PRINGGO WIDYO LAKSONO

PHD Dissertation

Electromyography (EMG) signal mapping and analysis based on upper-limb motion for controlling robotic arm

Pringgo Widyo Laksono

Ph.D advisor : Professor Minoru Sasaki, Dr. Eng

Co-Ph.D advisor : Professor Kojiro Matsushita, Dr. Eng

Ph.D Program in Production and System Development Engineering

Department of Mechanical and Civil Engineering

Gifu University

Acknowledgment

With the blessing of the mighty Allah SWT, I express my gratitude to God for his grace. Prayers and sholawat to our glorious lord prophet Muhammad SAW. Best wishes and all the best to my mother (Tri Sunarni), all my parents, and my father (Drs. Wiyanto) who passed away.

I am writing to express my heartfelt greatest gratitude for being the most influential professor, supervisor, and advisor, Senior Professor Minoru Sasaki, Dr. Eng. and the co-supervisor Professor Kojiro Matsushita, Dr.Eng., for their kindness and support during my 3 years of pursuing Ph.D. degree. There are many experiences and knowledge that I have learned during the 3 years of studies in Sasaki and Matsushita laboratory. I have been accepted as a laboratory member since 2018 and finally given the opportunities to finish my studies as a Ph.D. student in 2021.

For that, I would like to express my highest gratitude toward my main supervisor, Professor Minoru Sasaki, and co-supervisor, Professor Kojiro Matsushita for their kind support and guidance. I also would like to extend my gratitude toward examiner Profesor Kazuaki Ito for greatly assisted in the research. Without their humble support, I would not be able to achieve a step in my future life dream which is to be a university professor.

Many thanks and love go to my lovely wife Novrita Wulansari for her true love, patiently care, and incomparable support through the years leading to the completion of my Ph.D degree. My dearest daughters, Selena and Aida, I am gratified to have incredible daughters like you. Both of you will always be my soul and spirit. Thank you so very

much for actually being such amazingly fabulous daughters to me. To all my brothers and sisters, we are thankful for supporting and motivating us sincerely. May Allah bless all of you!

Then, I also would like to express my gratitude to all my laboratory colleagues including B4, M1 and M2 students. Notably, the Ph.D. students that have graduated from the laboratory and those currently still studying hard in Ph.D. studies. Those mentioned include: Paul Waweru Njeri(2019), Titus Mulembo Murwa(2019), Muhammad Syaiful Amri bin Suhaemi(2020), and Muguro Joseph Kamau. To all Engineering Faculty members UNS especially Industrial Engineering Dept, I am happy to have you in the group. Thank you for being my family that has been looking for. I am grateful.

I also want to include my gratitude to the organizations that I received sponsorship during my studies at Gifu University. Advanced Global Program (AGP) Gifu University has supported me with tuition waivers, entrance fees, and research assistant (RA) during my Ph.D. study (2018-2021). Financial support allowance from DIPA Universitas Sebelas Maret (UNS) Indonesia for supporting my living cost. Finally, the former head of department Industrial Engineering (IE) UNS (Prof Dr Wahyudi Sutopo, ST, M.Si), head department IE UNS Dr. Eko Liquiddanu,ST,MT., Dean Faculty Engineering, Vice Rectors , Rectors of UNS and Minister of Culture and Education of Republic Indonesia (RI) for allowing me to study abroad.

Abstract

Dependency on machines has been on an increasing trend in the last decade as applied in human daily task. In the future, human and machine collaboration will continue deepening with increased average amount of time spent for daily or work tasks. The use of human and robot interaction (HRI) has turned to be integral part of society, especially, in service area, health and clinical application, industrial purposes to mention but a few. The challenge this research seeks to understand the relationship between human muscle motions and joint angle motions. This is important to get intuitive EMG interface for robotic arm, but it is difficult to correspond between muscle and joint angle motion also robot and human are mechanically different.

The main focus of this research is to investigate the minimum analysis method for 3 upper-limb EMG signals to control 2 DoF robot arm. There are two objectives: (1) To measure 3 kinds of elbow & shoulder movements with 3 EMG sensors can be discriminate with simple EMG amplitude analysis; (2) To investigate the most simple and best analysis combination of feature extractions and machine learnings. To this end, these experiments were conducted to ascertain the validity of the approach.

The first experiment sought to address issues related to human-robot cooperation tasks focusing especially on robotic operation using bio-signals. In particular, this research proposes to develop a control scheme for a robot arm based on electromyography (EMG) signal that allows a cooperative task between humans and robots that would enable teleoperations. A basic framework for achieving the task and conducting EMG signals analysis of the motion of upper limb muscles for mapping the hand motion is presented. The objective of this work is to investigate the application of a wearable EMG

device to control a robot arm in real-time. Three EMG sensors are attached to the brachioradialis, biceps brachii, and anterior deltoid muscles as targeted muscles. Three motions were conducted by moving the arm about the elbow joint, shoulder joint, and a combination of the two joints giving a two degree of freedom. Five subjects were used for the experiments. The results indicated that the performance of the system had an overall accuracy varying from 50% to 100% for the three motions for all subjects. Subject 1 have an overall accuracy at 83.3%, subject 2 at 80%, subject 3,4 and 5 are 73.3%, 83.3% and 63.3% respectively. Motion 1 get highest accuracy 100%, beside motion 2 get lowest 50%. Subject 5 had the lowest accuracy at 63.3%. This study has further shown that upper-limb motion discrimination can be used to control the robotic manipulator arm with its simplicity and low computational cost.

The second research focuses on the minimum process of classifying three upper arm movements (elbow extension, shoulder extension, combined shoulder and elbow extension) of humans with three electromyography (EMG) signals, to control a 2-degrees of freedom (DoF) robotic arm. The proposed minimum process consists of four parts: time divisions of data, Teager–Kaiser energy operator (TKEO), the conventional EMG feature extraction (i.e., the mean absolute value (MAV), zero crossings (ZC), slope-sign changes (SSC), and waveform length (WL)), and eight major ma-chine learning models (i.e., decision tree (medium), decision tree (fine), k-Nearest Neighbor (KNN) (weighted KNN, KNN (fine), Support Vector Machine (SVM) (cubic and fine Gaussian SVM), Ensemble (bagged trees and subspace KNN). Then, we compare and investigate 48 classification models (i.e., 47 models are proposed, and 1 model is the conventional) based on five healthy subjects. The results showed that all the classification models achieved accuracies ranging between 74%–98%, and the processing speed is below 40

ms and indicated acceptable controller delay for robotic arm control. Moreover, we confirmed that the classification model with no time division, with TKEO, and with ensemble (subspace KNN) had the best performance in accuracy rates at 96.67, recall rates at 99.66, and precision rates at 96.99. In short, the combination of the proposed TKEO and ensemble (subspace KNN) plays an important role to achieve the EMG classification.

In conclusion, the validity of the usage of biological signals in robot control has been verified. Three EMG signals generated from three EMG sensors that are mounted at three different muscles that correspond with three upper-limb motions have been discriminated and applied successfully for controlling the robotic arm. Based on the model's discrimination generated from the EMG signals with simple feature extraction (Area), the result shows that 1 joint motion is easily discriminated (80-100%), however 2 joint motion is not easily discriminated (60-70%). The control scheme in use proofed to be manageable with an accuracy range between 50% to 100%. More than 2DoF motions need to analyze time-variation characteristics. The percentage of accuracy rate per subject ranged 63.3%-83.33%. The highest performance was motion 1 at 100% while the worst performance was motion 2 at 50%. The machine learning model function control shows promising contributions in a robust control that adapt to the usability of the controlling robotic hand. This can give better performance to control the robot and to tackle the limitation of the systems. Overalls, 48 classification models for discriminating three EMG signals at three upper limb motions and compared and evaluated the minimum parameters of feature extractions and machine learning models with five healthy subjects' data. The results showed that all the proposed models achieved accuracy rates in the range of 74%–98% and the processing speed was below 40 ms, which is an acceptable delay for

controlling a robotic arm. The most simple and best analysis combination of feature extractions and machine learnings is discrimination model with no division, using TKEO, using feature extraction (MAV,ZC,WLand SSC) and using ensemble subspace KNN. The performance index are accuracy rates 96.67% %, recall rate 99.66%, and precision rates 96.99%. Machine Learning “Ensemble (Subspace KNN)” seems to be effectively working for the 3 upper-limb EMG to 2DoF Robot arm Control. The difference between the best model and the conventional model was TKEO. It seemed that TKEO functioned to make the results of MAV, ZC, SSC, and WL stand out. Further research will deal with classifying more than three upper motions with three EMG sensors.

List of figures

List of tables

Table of Contents

Chapter 1 Introduction

1.1 Motivation of the research

In the recent past, robots have turned to be an integral part of the society with applications in industrial processes and manufacturing, military, welfare and healthcare systems, transportation, and autonomous vehicles, to name a few[1]–[3]. Robots in automation are fueled by the inherent virtue of machines in doing monotonous tasks with repeatable precision over a lengthy duration. In contrast to human labor, robots require fewer safety precautions, which makes them ideal for handling dangerous elements and disasters [1]–[3]. As an application area, the COVID-19 pandemic that has hit the world is a good case for the usage of robots in monitoring and delivery of essential services safely without compromising the safety of the medical staff [3], [4]. Research and development of the technology essential for estimating and identifying the usable biological signals through sensors and signal processing techniques, as well as their conversion into control scheme has been carried out in the recent past. The need for bio-signal control is heightened by elderly and disabled people who through myriad of happenstances have lost control of the environment[5]. The use` of non-physical interactions between humans and robots has grown rapidly in recent years. Human and robot cooperation trigger the development of research and technology in the bio-signal field.

Monitoring and analysis of bioelectrical signals and movements can help identification, prevention, and evaluation of a wide range of issues, especially in healthcare and industry[6]. Bio-signal such as Electromyography (EMG) is a pure source for driving human muscles that originate from the nerve center. EMG will play an

important role in the future, the prediction of global EMG usage and demand from 2020-2025 shows an increase in Compound Annual Growth Rate (CAGR) of 10.1% (mordorintelligence.com). The technological development of the EMG system and its use in the health sector, where EMG is a diagnostic procedure to evaluate the health condition of the muscles and nerve cells involved in moving the muscles. EMGs signal translates information into a number or graphic that can be processed into information.

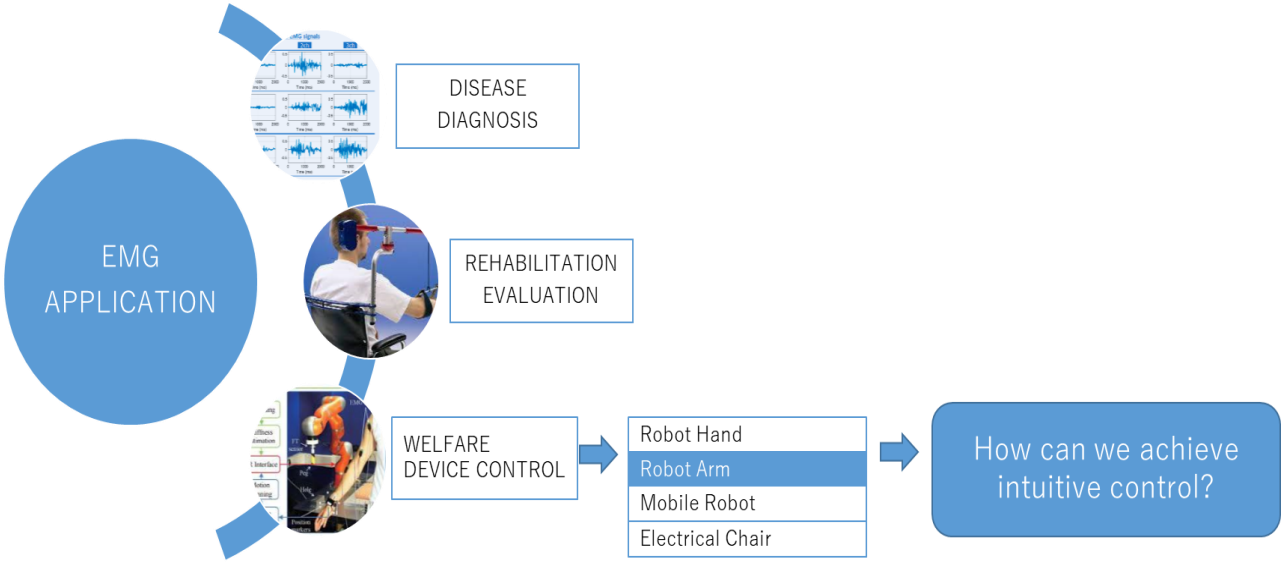

Figure 1-1 Application of electromyography

Human-Robot interface for robot arm should be more intuitive. It can be, a human arm motion directly control a robot arm. However, a robot arm and human are different. It is difficult to match between human and robot joint angles. Human joint angle is generated by muscles, so it is important to understand the the relationship between human muscle motion and robot motion (see fig.1).

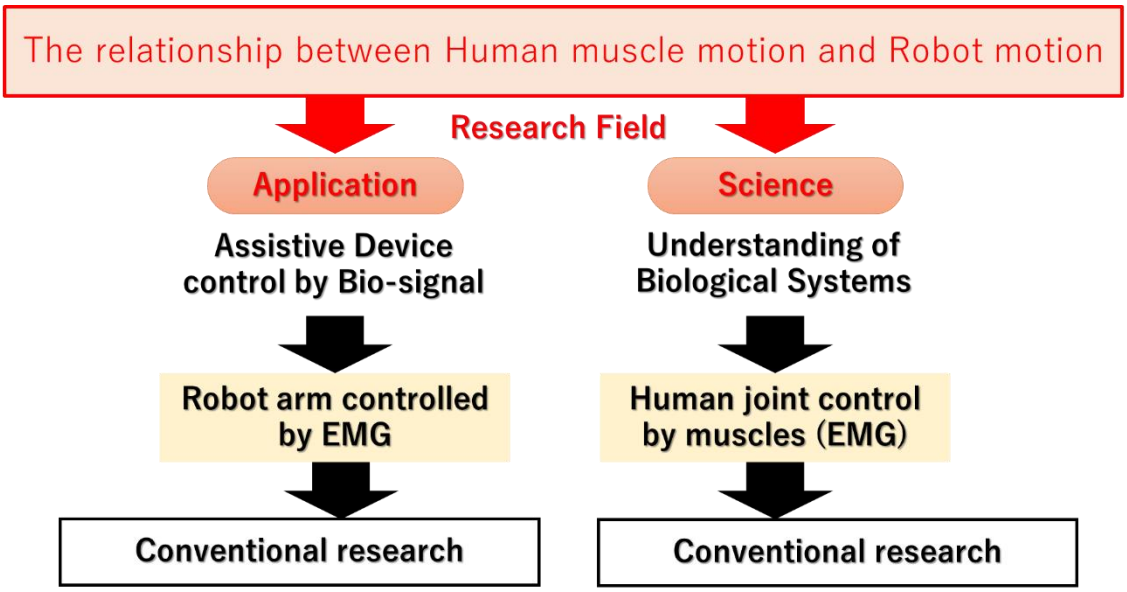

Figure 1-2. The relationship Human muscle motion and robot motion

Human Robot Cooperation (HRC) focuses on cooperative usage of either workspace, control scheme, or task completion. From the literature review, much more fine-tuning of the current robot system is needed to integrate robots in daily lives without being overly intrusive [2], [7], [8]. Attempts like the miniaturization of robots to fit in human workspaces is a step pursued by developers to achieve this integration. This context, called agent autonomy, closely considered leader-follower relationships that express how much robot motion is directly determined by humans for conducting tasks [9], [10].

1.2 State of the art of the research

Biopotential signals have been proposed to control robots in literature. Fukuda et al.[11] conducted teleoperation involving a human-assisted robotic arm using EMG signals. The systems used six EMG channels and a position sensor to capture grasping and manipulation signals. Artemiadis and Kyriakopoulos[12], [13] proposed a

methodology for controlling an anthropomorphic robot arm in real-time and high accuracy using EMG of the upper limb using eleven muscles and two-position tracker measurements. Benchabane, Saadia, and Ramdane-Cherif [14] introduced a new algorithm for real-time control of five prosthetic finger motions and developed a simple and wearable myoelectric interface. Liu and Young [15] proposed a practical and simple adaptive method for robot control using two channels for conducting upper-arm motion. Junior et al.[16] proposed a surface EMG control system to control the robotic arm based on the threshold analysis strategy. In their proposal, the EMG signal was acquired and processed by a conditioning system using Matlab software that gives flexibility and a fast way to reconfigure the settings for controlling an actuation system device.

1.3 Problem Statement

One of the significant aspects of HRC is the control mechanism employed. Conventionally, interaction with a robot is achieved with physical joysticks, keyboards, and other hardware systems [5–8,13]. The limitation with this input system is the level and quality of interactivity since they need to be physically attached. An alternative to this provision is the use of wireless and wearable devices. Wireless and wearable devices as a means of robot interaction open the control scheme to be versatile and user-friendly. In this research, the wearable control system was employed as it availed advantages, as is discussed below. With the advent of computing technologies, fine-tuned wearable devices have hit the market.

Of particular interest to the discussion is devices that can record physiological signals and process it to give meaningful information like heart rate, muscle activities, and such. All such signals emanating from the human body, jointly referred to as

biopotential signals, are present in the human body and can be integrated to enhance the quality of life [14–17]. Particularly so, in cases where there is a physical inability, bio-signals have been applied to restore control to patients and disabled individuals as well. An example of this is the use of prosthetics. Integrating such high-end devices with an HRC system would be advantageous in the versatility and universality of the control schema. 1 upper-limb muscle to 1 joint motion (elbow) with several feature extractions & machine learning process have been done. Many muscles (more than 5 muscles) to several joints motions with several feature extraction & machine learning also have been conducted by many researcher. In this research, we present one of the readily available signals from the skin surface, electromyography (EMG).

The position of the sensors on the surface of the muscles and its relations with the movements raised appears to be a challenge. How to perform motion mapping using several predefined sensors to get an EMG signal gathered from the movements of the elbow and shoulder joints. Although previous research on robot control using EMG signal amplitude has been done a lot. To control different functions, the user still has to switch between the available modes using a signal trigger[17]. Even though the control algorithm is quite robust, the results still show control limitations and are not intuitive for the end-user. Besides, the performances are still not good, such as accuracy and processing speed for real-time control[18].

1.4 Research Objectives

The objectives of this research is to map EMG signal that generated from elbow and shoulder movements in order to control robotic manipulator. There are two objectives: (1) To measure 3 kinds of elbow & shoulder movements with 3 EMG sensors

can be discriminate with simple EMG amplitude analysis; (2) To investigate the most simple and best analysis combination of feature extractions and machine learnings.

1.5 Research Contributions

The contribution of this study are the development of a control scheme for a robot arm based on the Electromyography and the influence of the position of the EMG muscle targeted and its relationship to upper-limb movements and the efficiency of classification model with minimum process using machine learninf. The targeted muscles are those that play an active role in the movement of the upper arm involving the elbow and shoulder joints. The initial hypothesis from this research is that the brachioradialis muscle (EMG channel 1/CH1) and biceps brachii (CH2) will play a role in movement 1, while the anterior deltoid muscle (CH3) will play a major role in motion 2 and motion 3. In addition, we confirmed that the classification model with no time division, with TKEO (Teager–Kaiser energy operator), and with machine learning method had good performance in accuracy rates, recall rates, and precision rates. In short, the combination of the proposed TKEO and ensemble subspace KNN(machine learning method) play an important role to achieve the EMG classification.

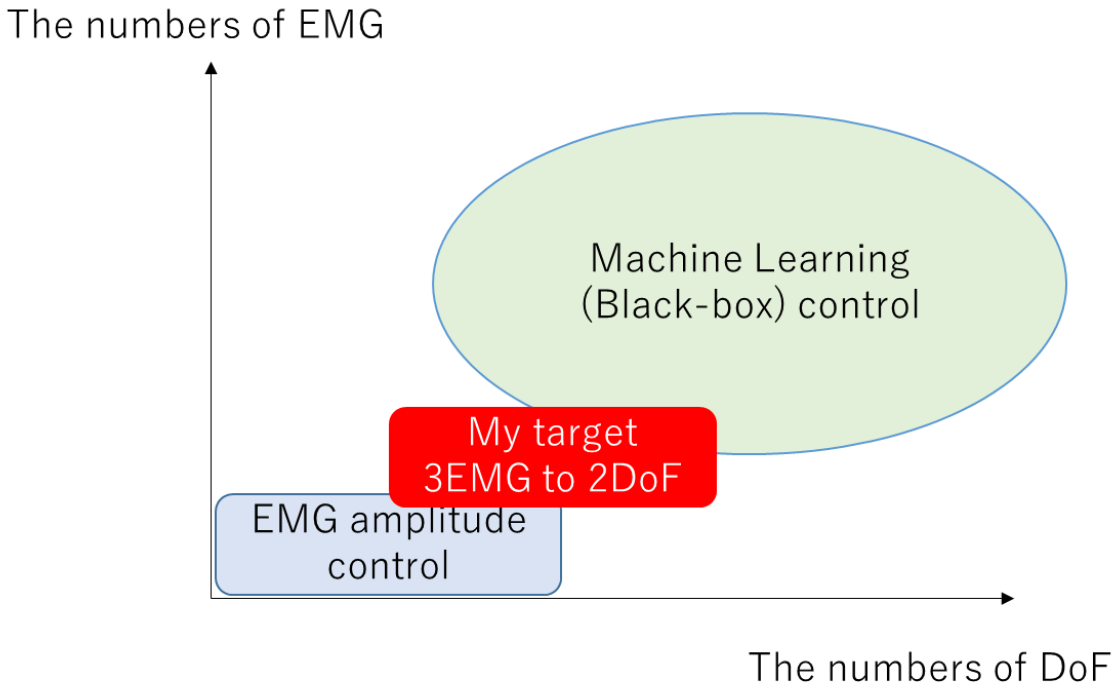

Figure 1-3 Research position of EMG control model based on numbers of EMG and DoF.

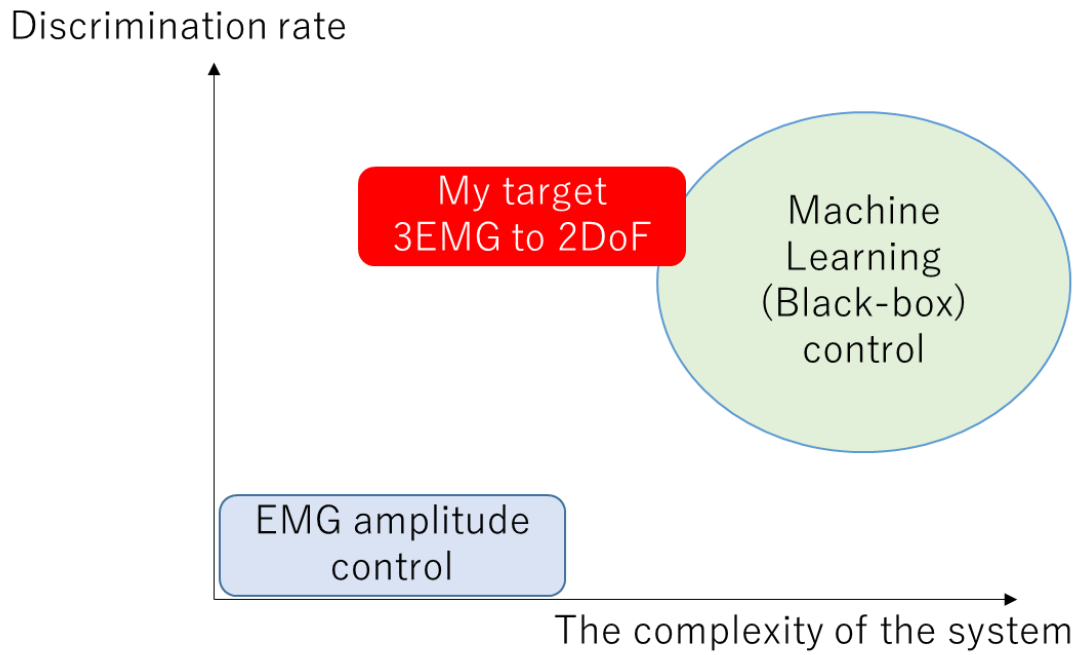

Figure 1-4 Research position of EMG control model based on discrimination rate and the complexity of the system

1.6 Outline of the thesis

The thesis writing structures based on the research objectives and its related information. There are six chapters in this thesis. In the first chapter is introduction, we will explain motivation of the research, state of the art of the research, problem statements, research objectives and contributions. In second chapter, we will explain the research methodology. Every information on research equipment, software, discrimination method, and other methodologies are discussed in detail. Chapter three is the first experiment in which we proposed mapping EMG signals generated by human elbow and shoulder movements to 2 dof upper-limb robot control. Chapter four is the second experiment where we proposed minimum process of EMG signals mapping using machine learning to improve classification performance. Finally, chapter five is the brief conclusion of this research

Chapter 2 Methodology

2.1 Proposed System Overview

Figure 2-1 illustrates an overview of the proposed control scheme. The system comprises of EMG signal acquisition system, processing unit, motion discrimination model/algorithm, and robot control mechanism. First, three target muscles were selected that are representative of arm muscle activity during motion. Data acquisition was performed on muscle surface using electrodes (Ag/AgCl, size: 57 x 48 mm, Biorode, Japan). A combination of three different motion comprising of single and double DOF were recorded.

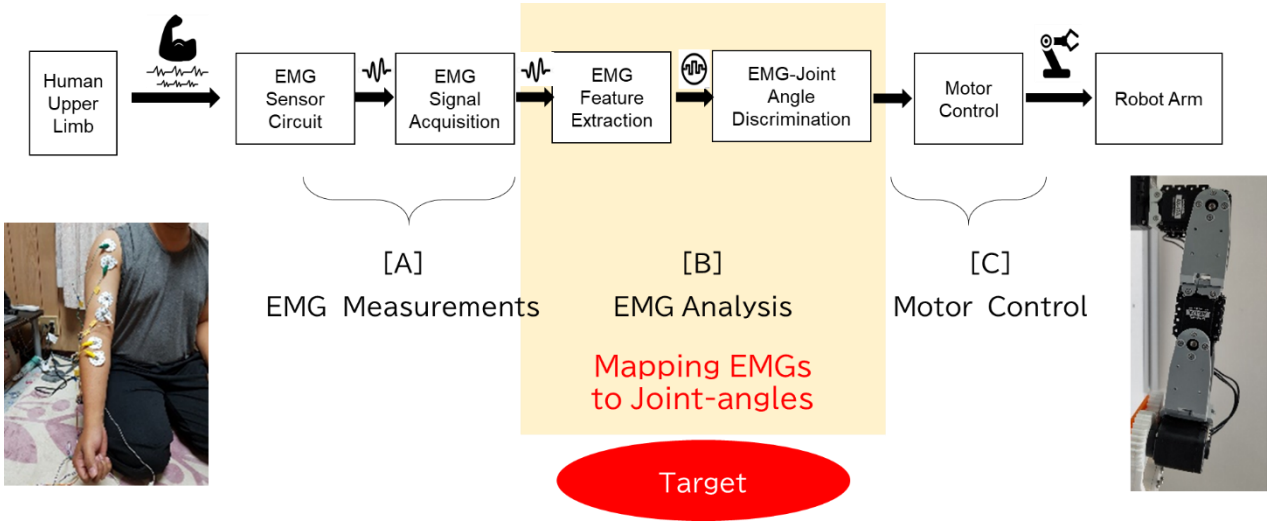

Figure 2-1. System overview of EMG signals mapping for controlling robotic arm

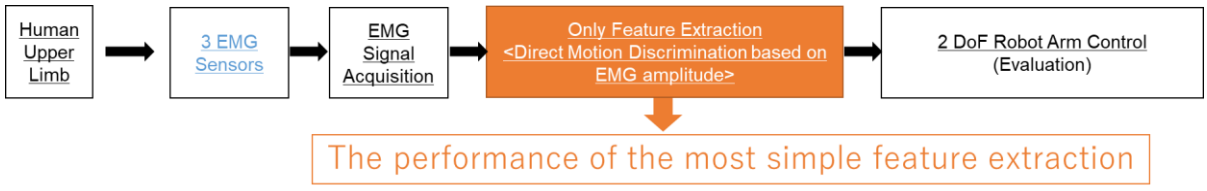

Figure 2-2. Proposed system with simple feature extraction

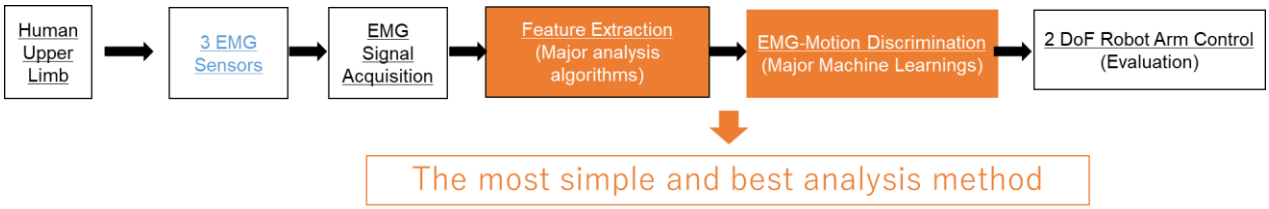

Figure 2-3 Proposed system with best simple model discrimination

2.1.1 EMG Measurement Device

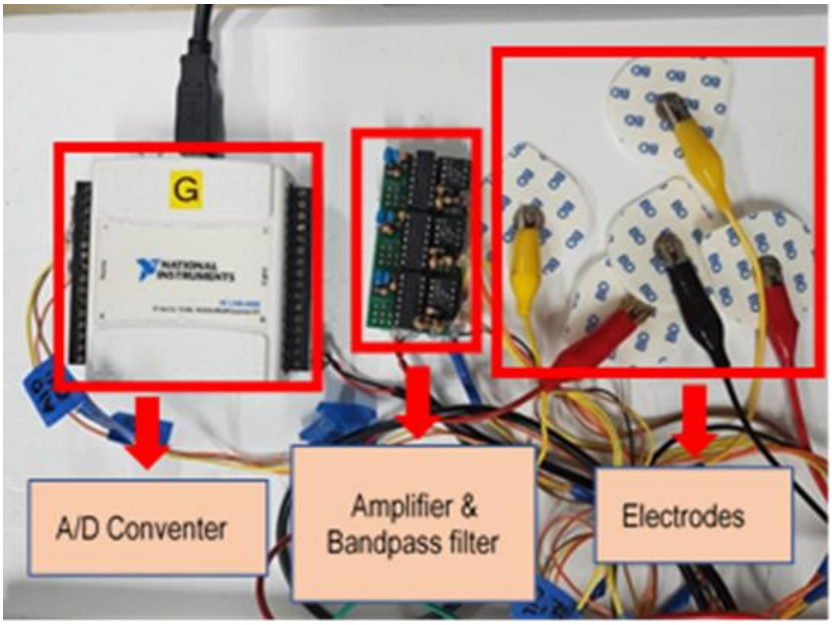

Figure 2-4 EMG measurements device.

Figure 2-4 displays EMG measurement system device. EMG measurement system featured a sensor circuit comprising of an instrumentation amplifier and an operational amplifier. The function of each component is as such;

1. **Disposable electrodes**: Measuring Direct-Current-EMG(DC-EMG) from the elbow and shoulder movement as the input signal. The input EMG from the selected muscles are is relatively small.
2. **EMG measurement circuit**: Amplifying the input signal to the designated range. A bandpass signal filtering method is also applied to convert the input DC-EMG signal

into Alternate-Current-EMG(AC-EMG) signal. In the research, we are utilizing the AC-EMG form of signal for EMG discrimination. The detailed schematic circuit can be found in figure 2-5.

3. **A/D converter**: Convert the amplified AC-EMG signal from the circuit into binary data. The binary conversion is to enable us to analyze the signal on a computer.
4. **Computer:** Analyze the EOG and EMG signal for discrimination and data saving.

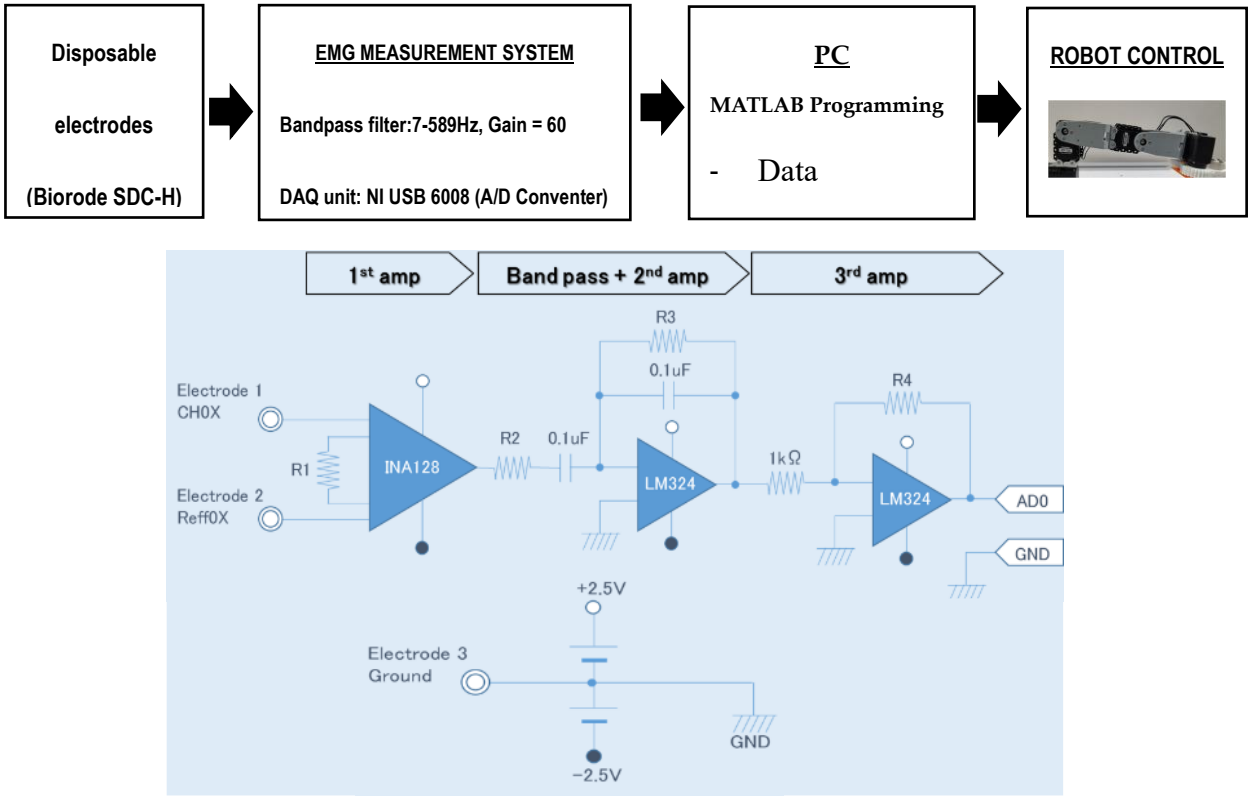

Figure 2-5 EMG measurements process and circuit schematic

The system comprises of EMG signal acquisition system, processing unit, motion discrimination model/algorithm, and robot control mechanism. First, three target muscles were selected that are representative of arm muscle activity during motion. Data acquisition was performed on muscle surface using pre-gelled silver chloride electrodes (Ag/AgCl, size: 57 × 48 mm, Biorode, Japan). A combination of three different motion comprising of single and double DOF were recorded.

The system employed an analog band-pass filter with a lower cut-off frequency of approximately 7 Hz and an upper cut-off frequency of 589 Hz and differential amplifiers' adjustable gain set to around 59-65 dB for each channel (see table 2-1). Data acquisition unit comprised of National Instruments (NI) Corporation USB-6008 for analog to digital conversion and a personal computer (PC) i5 2.7 GHz Let' note Panasonic. In the offline mode, signals were acquired at a sampling rate of 2 kHz. We used MATLAB® software for subsequent signal processing.

Table 2-1 The amplification value and the gain for EMG measurement.

Content	1st Amplifier	Bandpass + 2nd Amplifier					3rd Amplifier	Final Output	
	Resistor R0 [Ω]	Filter type	Cut-off Frequency [Hz]	Resistor R1/R2 [Ω]	Capacitor C1/C2 [F]	[uF]	Resistor R3/R4 [Ω]	Amplification Factor	Gain[db]
Value	1000	High-pass	7.23	2200	0.00001	10	15000	920	59
		Low-pass	589.46	2700	0.0000001	0.1	1000		
Amplification Factor	50.0	1.2					15		

2.1.2 Software MATLAB

Matlab has been used primarily to analyze signals such as EMG data. The abundance in mathematical functions and signals analysis can be handled by Matlab easily and simple.

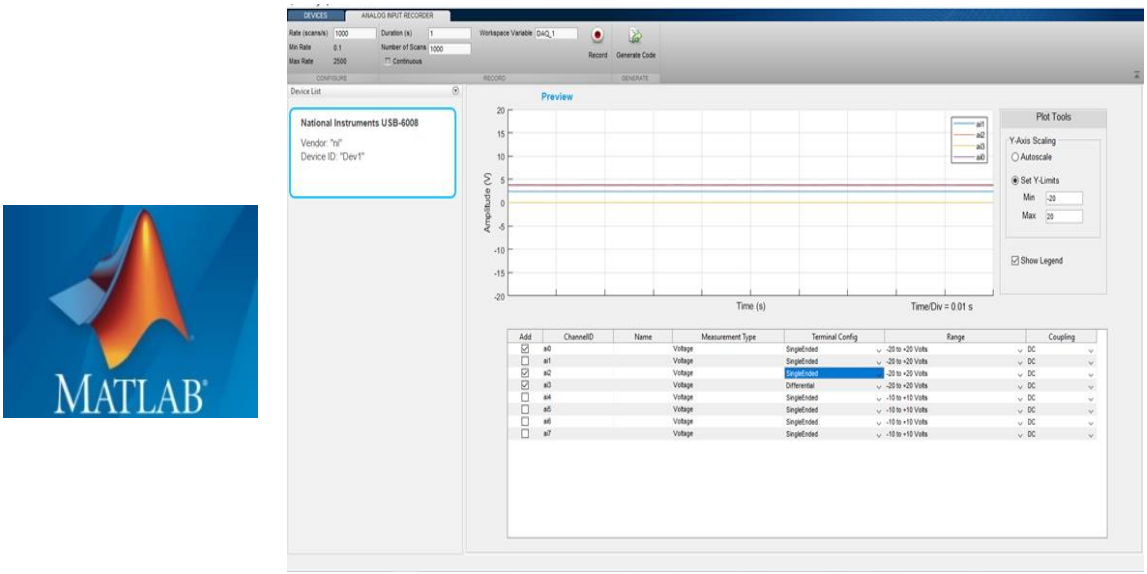

Figure 2-6 Signal Acquisition by Matlab NI-DAQ Acquisition 2019a

Data analog recorder application in Matlab that connected with NI-Daq is used to record EMG signal. The matlab based programming is not only use for recording, but also for reading the EMG signal data from the NI-Daq device, and also for processing the signals (see figure 2-6). Besides, the software is supported to control smart actuator such as Dynamixel 12A. The robot operation based on EMG has been developed using Matlab 2019a software.

Figure 2-7 Signals Analyzing using Matlab signal processing toolbox.

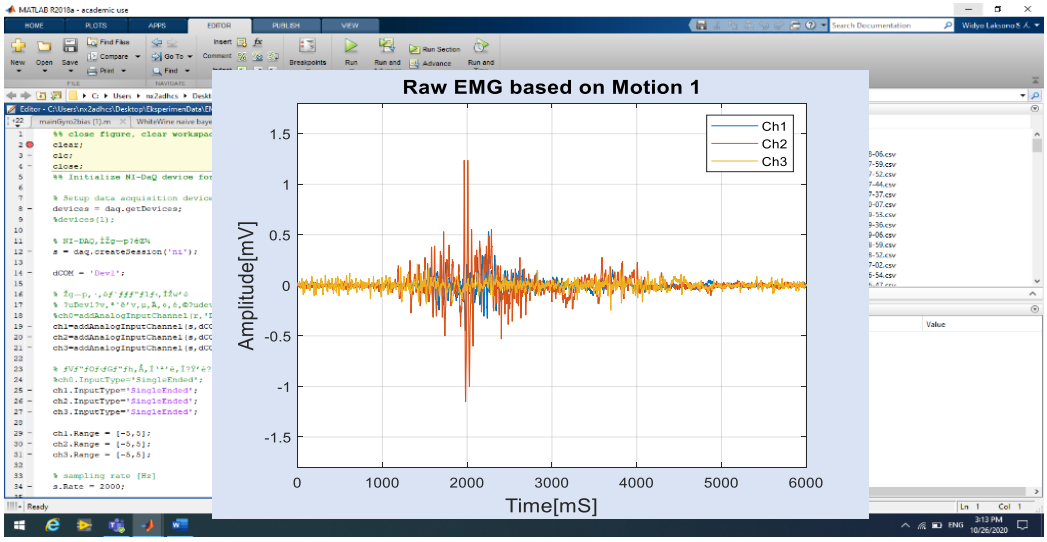

Figure 2-8 Graph plotting using Matlab 2019a

Matlab has been used mainly to analyze the bio-signals such as EMG data. The abundance in mathematical equations and toolboxes in Matlab made the data analysis became simple and easy. Moreover, Matlab gives an interactive graph plotting. All experimental graph shown throughout the paper is based on Matlab graph plot. Figure 2-8 displays the image of the graph plotting on the Matlab.

2.1.3 Muscles Position and Electrode Attachment

Although basic technique of surface Electromyography (SEMG) have been developed in twentieth century and SEMG become popular in last decade, SEMG do not still a general used technique. There are many variety and development of the method have taken place scattered over the world in specific scientific communities. Standardization is important. The SENIAM project (Surface EMG for the Non-Invasive Assessment of Muscles) is a European concerted action in the Biomedical Health and Research Program (BIOMED II) of the European Union. This project resulted standard recommendation for sensors and sensors placements procedures and signals processing methods for surface EMG, a set of test signals, books, publications etc.

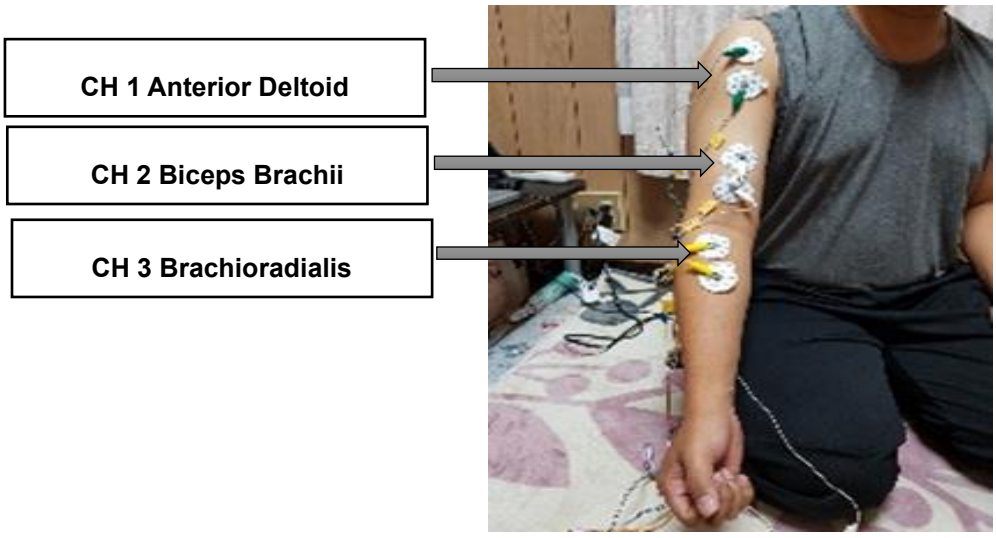

Figure 2-9 Muscles position and sensors placements

Targeted muscles were selected, incorporating the motion which is applied. EMG signals were captured from Brachioradialis, Biceps Brachii, and Anterior Deltoid muscles using bipolar electrode placement and one common electrode as reference (ground) placed on the bony part of the elbow as shown in figure 2-9.

This experiment used pre-gelled bipolar EMG sensor that mounted and placed

on the targeted muscles. We used SENIAM recommendation as standard procedures including how to clean the skin and to place the sensors. There are three major muscles that used in the first experiment. The anterior deltoid, biceps brachii and brachioradialis are selected as targeted muscles to be observed (see fig. 2-9). For each muscle, the electrodes need to be placed at one finger width distal and anterior to the acromion and the orientation direction of the line between the acromion and the thumb. By carefully attach the electrode, we could standardize the electrode placement for the test subject in experiments and reduce the inconsistency of the signal to be analyzed.

2.2 EMG Analysis

2.2.1 Pre-processing EMG Signal

The experimental setup involved multichannel EMG signal detection. Control is achieved by the introduction of a threshold to discriminate the state of muscle activation. The signals were processed with a conventional signal processing start from classical EMG signal acquisition, EMG feature extraction, and EMG motion mapping/model (see figure 2-10).

The acquired raw EMG signal was first processed to remove zero-offset, rectified, and filtered to smoothen the signal. Although the necessary analog filter already performed in the EMG measurement device, digital filter processing, as recommended by the previous researcher[19]–[21] was conducted. The band-pass filter having a bandwidth of 10-400 Hz was applied using the MATLAB signal processing toolbox to remove high random frequency interferences, noise introduced in the digitalization process, and remaining low-frequency noises from the motion artifacts, etc.

Processing of the raw data is critical to remove baseline noises, motion artifact noises, etc. An essential part of this paper is the analysis of the EMG signal. The acquired signal is passed through equation 1 for rectification and smoothing (by moving average) as shown equation (1) below.

$$Y[n] = \frac{1}{M} \sum_{i=-m}^{M} \left| |x[n+i]| \right| \tag{1}$$

Where M is the smoothing window size, and n is the current sampling point, x is the raw EMG signal from DAQ. The output Y[n] represents the processed EMG signal of the anterior deltoid, biceps brachii, and brachioradialis muscles, respectively[22]. After getting the processed EMG signal, the signal was normalized to obtain a uniform distribution discernable by a specified threshold. Equation (2) shows the operation.

$$EMG_{norm} = \frac{Y[n] - Y[n]_{(min)}}{Y[n]_{(max)} - Y[n]_{(min)}} \tag{2}$$

Where $Y[n]_{(min)}$ is the minimum value of the processed signal, and $Y[n]_{max)}$ is the maximum.

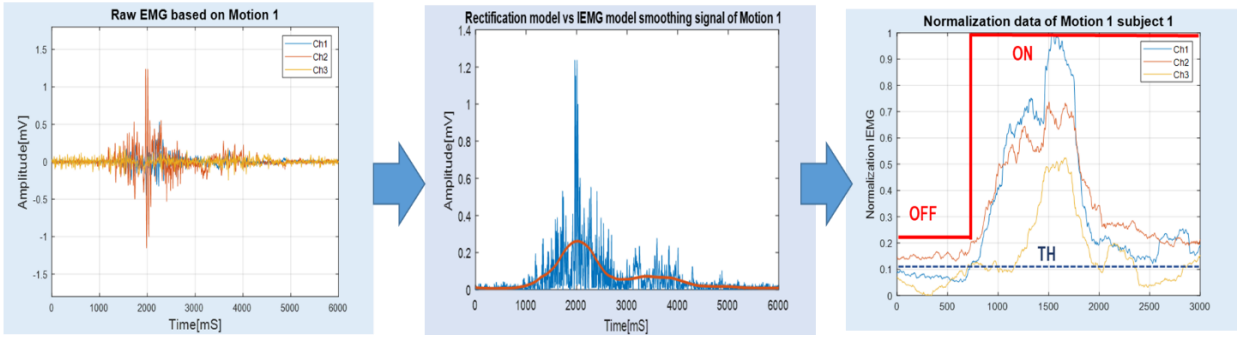

Figure 2-10 EMG Signal processing illustration phase

Discrimination of active motion was done by identifying different features of

three EMG channels (Ch1, Ch2, and Ch3), see figure 2-11. In this case, we used the features as the control parameters. Three control parameters were applied; the mean of the envelope signal, the maximum value of the amplitude, and the area under the curve. These steps consisted of how to overcome the desired output from the signal features. As earlier mentioned, to discriminate the activation state of the muscles from each channel, we proposed the threshold method.

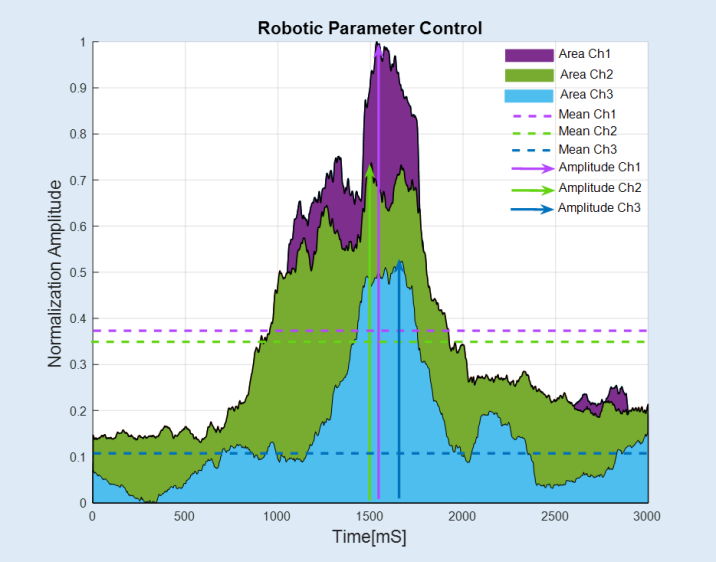

Figure 2-11 Robotic parameter control

The control parameters determine whether the threshold will be activated or not. The threshold method determined muscle activation state (MS), which was expressed as muscle activation (ON) or muscle deactivation (OFF). The ON state was returned if the signal was above the baseline threshold of the envelope signal whereas, an OFF state resulted whenever the rectified signal was below the baseline threshold. The choice of the threshold was advantageous in aiding the removal of any residual noise of the envelope signal [23]. The muscle state is defined as in (3):

$$MS(n) = \begin{cases} 1(ON) \; if \; EMGnorm > Th \\ 0(OFF) \; else \end{cases} \tag{3}$$

Where EMGnorm is represented as normalized and filtered EMG signal and n represent either channels 1, 2, or 3 of EMG. To evaluate the performance of the controlling parameter, the successful mapping rate at the times that the robot arm mimics the motion of the subject's upper-limb motion correctly out of the total number of trials was determined.

2.2.2 Feature Extraction

Feature extraction employed in this research was in time-domain. The method is often used because of its quick and simple implementation. Time-domain features are processed without any signal transformation for the raw EMG signals and evaluated based on the value of signal amplitude that varies over time[1], [24]–[29]. The statistical properties of EMG are always changing over time. However, researchers still prefer to use time domain features because their computational is less complex as compare to those of the frequency domain features [29]–[31].

Integrated EMG (IEMG) or also called Integrated Absolute Value (IAV) : IEMG /IAV is normally used as an onset detection index that is related to EMG signal sequence firing point. IEMG is the summation of the absolute values of EMG signal amplitude, which can be expressed as follow:

$$IEMG = \sum_{i=1}^{M} |Xi| \quad (4)$$

Mean Absolute Value (MAV) is similar to IEMG that normally used as an onset index to detect the muscle activity. MAV is the average of the absolute value of EMG signal amplitude. MAV is a popular feature used in EMG hand movement recognition application. It is defined as

$$MAV = \frac{1}{M}\sum_{i=1}^{M}|Xi| \quad (5)$$

Variance (VAR) captures the power of EMG signal as a feature. Normally, variance is mean of square of deviation of that variable. However, mean value of EMG signal is close to zero. Therefore, variance of EMG signal can be defined as

$$VAR = \frac{1}{M-1}\sum_{i=1}^{M}Xi^2 \quad (6)$$

Root Mean Square (RMS): RMS is related to constant force and non-fatiguing contraction. Generally, it similar to SD, which can be expressed as

$$RMS = \frac{1}{M}\sum_{i=1}^{M}Xi^2 \quad (7)$$

Waveform length (WL): WL is the cumulative length of waveform over time segment. WL is similar to waveform amplitude, frequency and time. The WL can be formulated as

$$WL = \sum_{i=1}^{M-1}|Xi + 1 - Xi| \quad (8)$$

Zero crossing (ZC) is the number of times that the amplitude values of EMG signal crosses zero in x-axis. In EMG feature, threshold condition is used to avoid from background noise. ZC provides an approximate estimation of frequency domain properties. The calculation is defined as

$$ZC = \sum_{n=1}^{N-1}[f(x_n - x_{n+1}) \cap |x_n - x_{n+1}| \geq threshold] \quad (9)$$

$$f(x) = \begin{cases} 1, & if\ x \geq threshold \\ 0, & otherwise \end{cases}$$

Slope Sign Change (SSC): SSC is related to ZC. It is another method to represent

the frequency domain properties of EMG signal calculated in time domain. The number of changes between positive and negative slope among three sequential segments are performed with threshold function for avoiding background noise in EMG signal. It is given by

$$SSC = \sum_{n=2}^{N-1}\left[f[(x_n - x_{n-1}) \times (x_n - x_{n+1})]\right] \quad (10)$$

$$f(x) = \begin{cases} 1, & if\ x \geq threshold \\ 0, & otherwise \end{cases}$$

2.3 Robot Control

The flowchart in figure 2-12 describes the flow from the beginning until the end of the robot control.

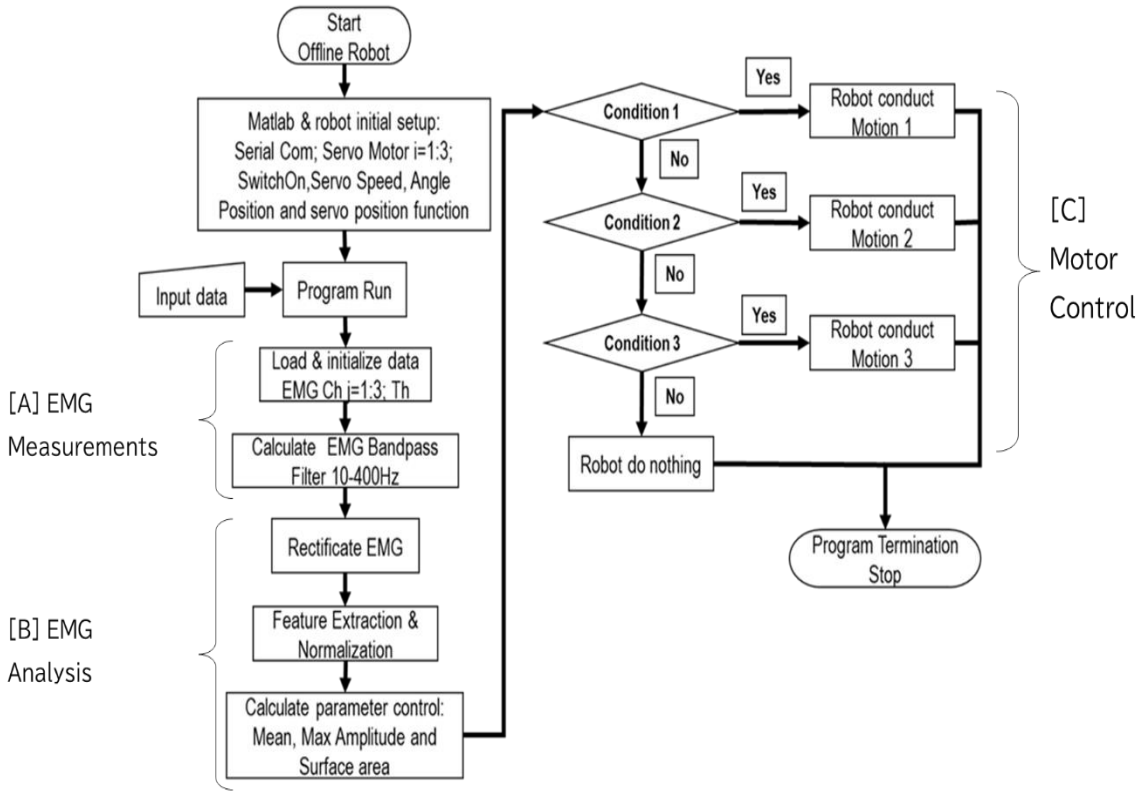

Figure 2-12 Flow chart offline robot control.

Custom assembled R-R-R (three revolute joints) configuration robot arm

illustrated in figure 2-13b, assembled from the Dynamixel unit was used in this research work for experiments. Dynamixel AX-12A is a smart actuator with a fully integrated DC servo motor module. The input voltage rating is around 9.0-12V, which can produce a speed of 59 rpm with θ rotation angle (max) of 300 degree, and resolution of 0.2930 deg/pulse. Four actuators were assembled as a robotic arm with two links and three joints, as shown in figure 2-13c. In this research, two motors are needed to move the robot joint according to the movement of the shoulder joint and elbow joint.

Robot-PC communication was achieved by using a serial connection between MATLAB and the motor controller connected to the computer via USB. Servo motor controller is a small size universal serial bus (USB) communication converter that enables the interfacing and operation of the actuators from the computer. It also supports 3 pin TTL connectors that used to link up with the Dynamixel motor.

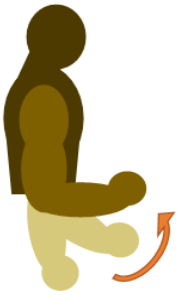

(a)Elbow motion

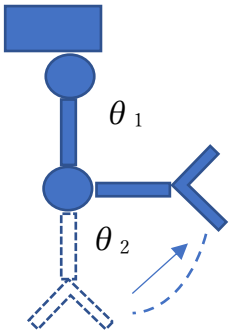

(b) R-R-R Robot configuration (revolute joints)

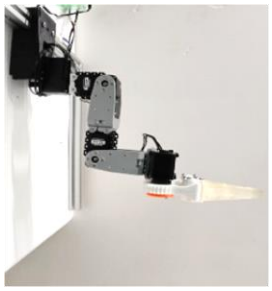

(c) Assembled Dynamixel robot arm (2 links and 3 joints)

Figure 2-13 Robot arm configuration.

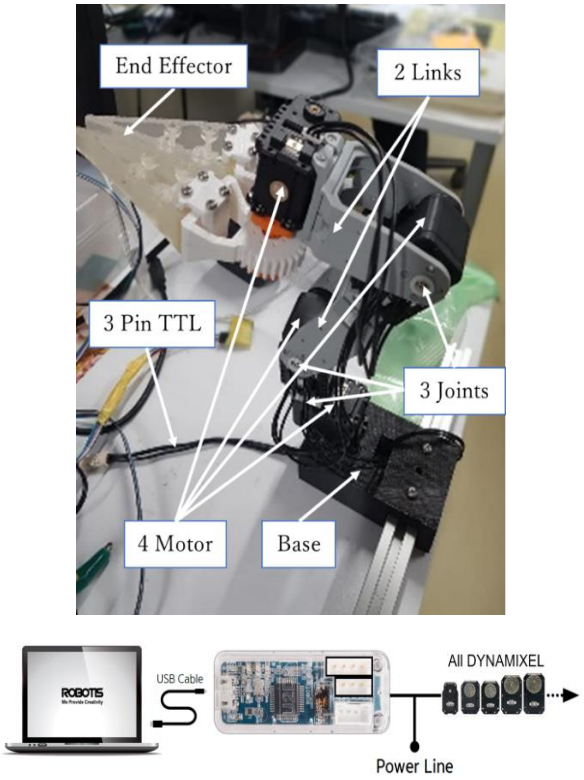

Figure 2-14 Robot and computer communication

Serial Communication (8 bit) is applied as protocol type connection (see fig. 2-14). U2D2 micro-B USB connected to the USB port of the PC with the enclosed USB cable. 3Pin TTL connector used to link up with Dynamixel's. An external power supply 12V should provide power to Dynamixel. reference baudrate is 115.200 with error 0.04.

2.4 Machine Learning Stage

Machine learning is a area in computer science where existing data are used to predict, or respond to, further data. Pattern recognition, computational statistics, and artificial intelligence are closely related by machine learning fields. Machine learning is important in areas like image recognition, filtering, classification, clustering, predicting, and others where it is to make decision, to write algorithms and to perform a task[32]. The main role of the machine learning module is to classify the patterns extracted from

the EMG signals into their respective movement. In this study, the classifications of EMG signals are done using major machine learning models (i.e., decision tree, k-Nearest Neighbor (KNN), Support Vector Machine (SVM), Ensemble from MATLAB statistic and machine learning toolbox (version 2019a).

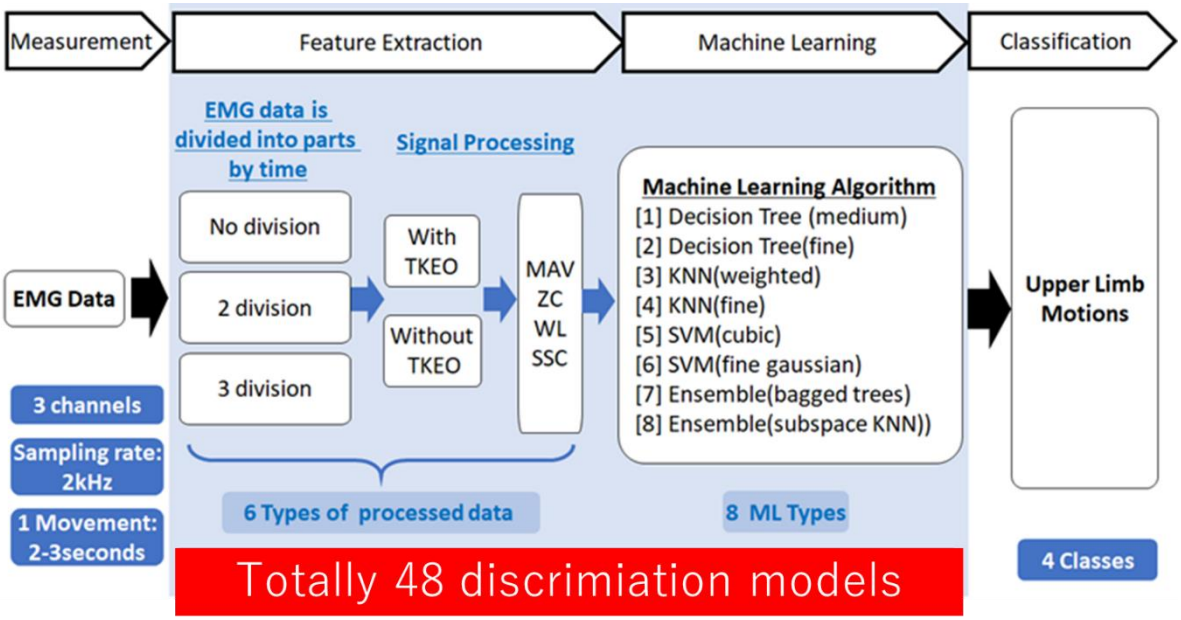

Figure 2-15 Proposed discrimination models for comparation.

Totally 48 discrimination models have been compared (see figure 2-15). There are combinations of EMG data contained 3 channels divisions, using with/without TKEO, feature extractions (MAV,ZC,WL and SSC) and 8 machine learning types.

Teager–Kaiser energy operator (TKEO) was used for enhancing the amplitude and frequency of TD EMG signals without converting those signals to the FD see figure 2-16 [41–43]. TKEO was performed to enhance muscle activation detection. TKEO requires only three samples to estimate the signal energy at each sample time, resulting in low computational demands, which even enables semi real time applications such as EMG driven (training) devices. TKEO as data preconditioning for autonomous burst

detection during real life.

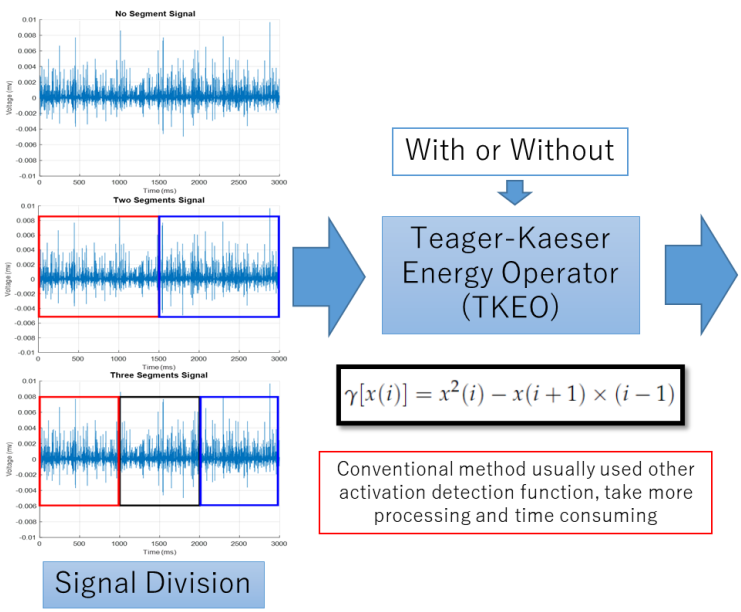

Traditional Feature Extractions

Feature Extraction Method	Contents
MAV	The average of the absolute value of EMG signal amplitude
Waveform length	The cumulative length of waveform over time segment / Similar to waveform amplitude, frequency and time
Zero crossing (ZC)	The number of times that the amplitude values of EMG signal crosses zero in x-axis
Slope Sign Change (SSC)	The frequency domain properties of EMG signal calculated in time domain

Figure 2-16 Pre-processing EMG Signal (Signal divisions and TKEO)

2.4.1 Decision tree.

A decision tree is a non-parametric methods with a similar structure to a tree-like graph used to make decisions. It has three kinds of nodes: decision nodes, chance nodes and end nodes. Decision trees, or classification trees and regression trees, predict responses to data. To predict a response, follow the decisions in the tree from the root (beginning) node down to a leaf node. The leaf node contains the response. Classification trees give responses that are nominal, such as 'true' or 'false'. Regression trees give numeric responses[32].

2.4.2 K-Nearest Neighbor

The others non-parametric supervised classification algorithm is called K-Nearest-Neighbors (KNN), which is effectivr yet simple in many cases. The KNN classifier is considered as one of the most popular classifier for pattern recognition due to

its effective performance with efficient results and its simplicity. It is commonly used in the ares of pattern recognitions, machine learning, text categorization, data mining, object recognition and others. KNN algorithm classifies by analogy i.e. by comparing the unknown data point with the training data points to which it is similar. Similarity is measured by Euclidean distance. The attribute values are normalized to prevent attributes with larger ranges from outweighing attributes with smaller ranges. In KNN classification, the unknown pattern is assigned the most predominant class amongst the classes of its nearest neighbors. In case there is a tie between two classes for the pattern, the class that has minimum average distance to the un-known pattern is assigned. Through the combination of a number of local distance functions based on individual attributes, a global distance function dist can be calculated. As given in equation 11, the simplest way is to sum up the values:

$$Dist.(X^T, X) = \sum_{i=1}^{n} dist\ A_i(A^T \cdot A_i, X \cdot A_i) \quad (11)$$

Where X^T is the test tuple, X is a nearest neighbor, and Ai (i=one to n) represents the attributes of the data points.

The weighted sum of local distances is known as global distance. The attributes A_i can be assigned specific weights wi to depict their level of importance in deciding the appropriate classes for the samples. The weights usually range between 0-1. Irrelevant attrib-utes are assigned a weight 0. Thus, equation (12) can be modified and written as equation:

$$Dist.(X^T, X) = \sum_{i=1}^{n} w_i \times dist\ A_i(A^T \cdot A_i, X \cdot A_i) \quad (12)$$

2.4.3 Support Vector Machines

Support vector machines are supervised learning models with associated learning algorithms used for binary classification. SVM used for classification and regression analysis. SVM training algorithm builds a model that assigns examples into categories. The goal of an SVM is to produce a model, based on the training data, that predicts the target values. In SVM nonlinear mapping of input data in a higher-dimensional feature space is done with kernel functions. In this feature space a separation hyperplane is generated that is the solution to the classification problem. The kernel functions can be polynomials, sigmoidal functions, and radial basis functions. Only a subset of the training data is needed; these are known as the support vectors[33]. The training is done by solving a quadratic program, which can be done with many numerical software programs such as Matlab.

2.4.4 Ensemble

A machine learning method that combines several base models in order to produce one optimal predictive model is called by Ensemble methods. This learning algorithm are build a set of classifiers and then classify new data points by taking a (weighted) vote of their predictions. Ensemble method is base on Bayesian averaging, but more recent algorithms include error-correcting output coding, boosting, and bagging[34]. This learning classfiers technique is a set of classifiers whose individual decisions are mixed in some way typically by weighted or unweighted voting to classify new data. One of the most active fields of research in supervised learning has been to study methods for constructing good ensembles of classifiers. The main finding is that ensembles are often much more accurate than a classifiers that make them rise.

2.5 Target Upper Limb Motion

Human upper-limb movement is one of the most complex motions and involves many components such as musculoskeletal, nerves, and others to support multiple degrees of freedom. The upper limb conducts many motions that require coordination of the joint, which consists of many ranges of motions for daily life tasks. To make the scope of the research more specific, we focus on the shoulder and elbow joints moving separately to represent single DOF movements and a combination of two joints to achieve multiple DOF. The combination of three motion gesture is as illustrated in figure 2-17. Shoulder motion allows three DOFs (i.e., abduction / adduction, flexion / extension, and internal / external rotation). Elbow motion has two DOFs (i.e., flexion / extension and supination / pronation)[21], [35].

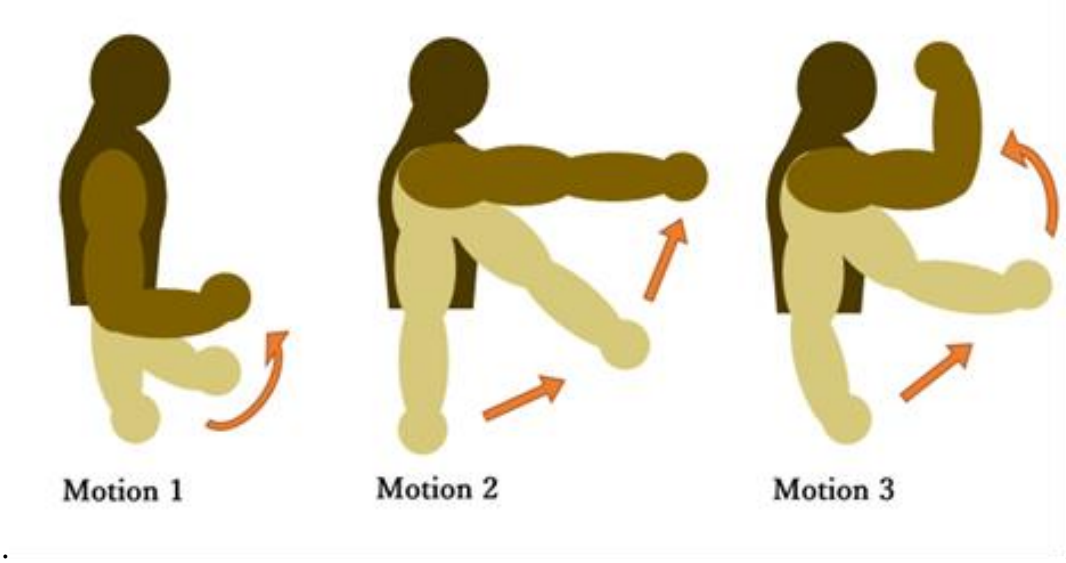

Figure 2-17 Motion illustration

Chapter 3 Mapping EMG signals generated by Human Elbow and Shoulder Movements to 2 DoF Upper-Limb Robot Control.

3.1 Background

In the recent past, robots have turned to be an integral part of the society with applications in industrial processes and manufacturing, military, welfare and healthcare systems, transportation, and autonomous vehicles, to name a few[1], [2]. Robots in automation are fueled by the inherent virtue of machines in doing monotonous tasks with repeatable precision over a lengthy duration. In contrast to human labor, robots require fewer safety precautions, which makes them ideal for handling dangerous elements and disasters[1], [2]. As an application area, the COVID-19 pandemic that has hit the world is a good case for the usage of robots in monitoring and delivery of essential services safely without compromising the safety of the medical staff [4].

Robots have been in use in various aspects of human life, as earlier mentioned. Regarding the control mechanism, modes of application of robot can be broadly categorized as autonomous, cooperative, and or hybrid mode[9]. Autonomous mode, in this case, is defined to capture all control schemes that do not require human intervention. This is the case in most industrial robots, as well as the highly anticipated autonomous cars. In cooperative mode, the robot is driven by human input where the robot act to respond or mimic the human input. An example of this scheme would be crane operation, robot control using joysticks, and others. The hybrid model would be a case where the robot has an element of autonomy as well as input control initiated by a human. In both

the hybrid and cooperative model, an element of human-robot collaboration (HRC) is present[12], [15], [36]–[38].

HRC focuses on cooperative usage of either workspace, control scheme, or task completion. From the literature review, much more fine-tuning of the current robot system is needed to integrate robots in daily lives without being overly intrusive[2], [7], [8]. Attempts like the miniaturization of robots to fit in human workspaces is a step pursued by developers to achieve this integration. This context, called agent autonomy, closely considered leader-follower relationships that express how much robot motion is directly determined by humans for conducting tasks[9],[12].

One of the significant aspects of HRC is the control mechanism employed. Conventionally, interaction with a robot is achieved with physical joysticks, keyboards, and other hardware systems[12], [15], [36], [37], [39]. The limitation with this input system is the level and quality of interactivity since they need to be physically attached. An alternative to this provision is the use of wireless and wearable devices. Wireless and wearable devices as a means of robot interaction open the control scheme to be versatile and user-friendly. In this research, the wearable control system was employed as it availed advantages, as is discussed below.

With the advent of computing technologies, fine-tuned wearable devices have hit the market. Of particular interest to the discussion is devices that can record physiological signals and process it to give meaningful information like heart rate, muscle activities, and such. All such signals emanating from the human body, jointly referred to as biopotential signals, are present in the human body and can be integrated to enhance the quality of life[5], [40]–[42]. Particularly so, in cases where there is a physical inability,

biosignals have been applied to restore control to patients and disabled individuals as well. An example of this is the use of prosthetics. Integrating such high-end devices with an HRC system would be advantageous in the versatility and universality of the control schema. In this paper, we present one of the readily available signals from the skin surface, electromyography (EMG).

Biopotential signals have been proposed to control robots in literature. Fukuda et al. [11] conducted teleoperation involving a human-assisted robotic arm using EMG signals. The systems used six EMG channels and a position sensor to capture grasping and manipulation signals. Artemiadis and Kyriakopoulos[12], [13] proposed a methodology for controlling an anthropomorphic robot arm in real-time and high accuracy using EMG of the upper limb using eleven muscles and two-position tracker measurements. Benchabane, Saadia, and Ramdane-Cherif [14] introduced a new algorithm for real-time control of five prosthetic finger motions and developed a simple and wearable myoelectric interface. Liu and Young[15] proposed a practical and simple adaptive method for robot control using two channels for conducting upper-arm motion. Junior et al. [16] proposed a surface EMG control system to control the robotic arm based on the threshold analysis strategy. In their proposal, the EMG signal was acquired and processed by a conditioning system using LabVIEW software that gives flexibility and a fast way to reconfigure the settings for controlling an actuation system device.

EMG signals are prone to interference by noises from power lines, electromagnetic radiation, cable movements, skin impedance, among others[15], [24], [43]. For this reason, signal processing is an indispensable step in the control algorithm. The general outline of the control algorithm can be described as follows. From targeted

muscle, the acquired raw EMG signal is conditioned to eliminate noise, relevant features are extracted, and finally, control is performed based on the resulting signal.

EMG control has been applied in various areas of robot control. The control systems in literature can be categorized as pattern and non-pattern recognition systems [37]. The pattern recognition system detects patterns and EMG signals associated with the task. This is the case in hand pattern recognition, finger patterns, and other systems proposed to recognize the current state of the hand [1], [8], [25]–[28], [30], [39]. On the other hand, nonpattern recognition controls are practical and often used as control schemes. The objective, in this case, is to characterize motion, gripping force, rotation of angles, and others [8], [11], [15], [19], [23], [28], [44], [45].

The main objective of this experiment is to investigate the application of wearable EMG device to control a robot arm in real-time. The focus is on EMG signal control corresponding to upper-limb motions of the arm and to analyze its relations. The control scheme is non-pattern recognition in nature, specifically ON/OFF control with threshold level control. This motivation for the usage of this scheme was informed by its simplicity and low computation cost. However, the method has been reported to have reduced accuracy compared with other pattern-based methods [25].

The authors in [46] proposed the use of pattern recognition control mechanism for a malfunctioning upper-limb prosthesis. In this control scheme, only a single degree of freedom (DOF) movement (hand open/close or wrist flexion/extension) was supported at any one time. This paper target multiple DOF with fewer electrodes on the upper limb. Besides, the limitation of the DOF, conventional amplitude-based control method has a slow response and takes time for the users to learn to contract/co-contract the targeted

upper-limb muscles[1], [22], [26], [27], [46].

In this research, the EMG signal corresponding to upper-limb motions consisting of elbow and shoulder joints is discriminated to control a robot arm applicable in the teleoperated robot cooperation system. A low-cost wearable embedded system was customized to conduct three motions corresponding to the motion of the elbow joint and shoulder joint in real-time to the robot manipulator. The robot manipulator is a compact serial communication robot and suitable for use in home or experiment environments. Three pairs of surface EMG sensors were mounted on the Anterior deltoid, Biceps brachii, and Brachioradialis as the target muscles

Three different motions were proposed for analysis; the elbow flexion as motion 1, shoulder flexion as motion 2, and a combination of elbow and shoulder flexion movement called the uppercut motion as motion 3. In the recording of the EMG signal, the upper limb of motion 1 and motion 2 are limited to a range of up to 90 degrees for modeling of the relation of EMG and joint angle. The contribution of this study is the development of a control scheme for a robot arm based on the Electromyography and the influence of the position of the EMG muscle targeted and its relationship to upper-limb movements. The targeted muscles are those that play an active role in the movement of the upper arm involving the elbow and shoulder joints. The initial hypothesis from this research is that the brachioradialis muscle (EMG channel 1/CH1) and biceps brachii (CH2) will play a role in movement 1, while the anterior deltoid muscle (CH3) will play a major role in motion 2 and motion 3.

3.2 Experiment

Five healthy, right-handed subjects (all males) with ages ranging from 20 to 40 years participated as volunteers for the experiment. All of them provided written informed consent following approval procedures (number 27-226) issued by Gifu University ethics committee. The issue is the application to motion intention estimation and device control based on biological signal measurement considering user-specific physical characteristics and environmental characteristics. The experiment was conducted with subjects seated comfortably in a chair with right arm rested (0-degrees). For familiarization, the participants performed several arm motions prior to recording as well as get a proper threshold for individual calibration.

During recording, the participants were instructed to raise and lower the arm (motion1) within 2 seconds. Every motion was repeated 10 times in offline mode. In online mode, the robot was moved with successive arm motion for visual feedback. The robot arm control was initially conducted in offline mode. The EMG data loaded as an input for controlling the robotic arm.

$$MS(n) = \begin{cases} 1(ON) & if\ EMGnorm > Th \\ 0(OFF) & else \end{cases} \quad (13)$$

From formula (13), if we represented MS(CH1) as A, MS(CH2) as B, and MS(CH3) as C, discrimination of the active motion is handled by the control algorithm with conditions shown in (14). Motion 1, motion 2, and motion 3 are deduced conditional manipulations of signals from the three channels. In particular, when the EMG signal from both CH1 and CH2 is above the baseline TH (threshold), and CH3 is below the threshold; the command to activate motion 1 is classified as ON, as shown in equation 14.

Similarly, if either CH 1 or CH2 is lower than the threshold and CH3 is higher than the threshold, then motion 2 is ON. Finally, motion 3 is solely dependent on all channels that are greater than the threshold.

$$If\ A\ > Th\ and\ B > Th\ and\ C < A\ then\ It\ is\ Condition\ 1$$
$$If\ A\ < Th\ or\ B < Th\ and\ C > Th\ then\ It\ is\ Condition\ 2 \quad (14)$$
$$If\ A\ > Th\ and\ B > Th\ and\ C > Th\ It\ is\ Condition\ 3$$

Table 3-1 Discriminating of EMG and robot angles.

EMG			**Upper-Limb**	**Robot Arm**	
CH1	**CH2**	**CH3**	**Status**	**Angle θ_1**	**Angle θ_2**
ON	ON	OFF	Motion 1	0°	90◦
OFF	ON	ON	Motion 2	90◦	0◦
ON	ON	ON	Motion 3	90◦	90◦
OFF	OFF	OFF	Do nothing	0◦	0◦

Table 3-1 reports the discriminations status for each EMG signal related to the movements of the robot arm. Angle θ_1 (shoulder joint) and θ_2 (elbow joint) are joint angles.

3.3 Results and Discussion

The following section describes the experiment, signal processing, and robot control model results. The output of the processed EMG is used for controlling the robotic manipulator.

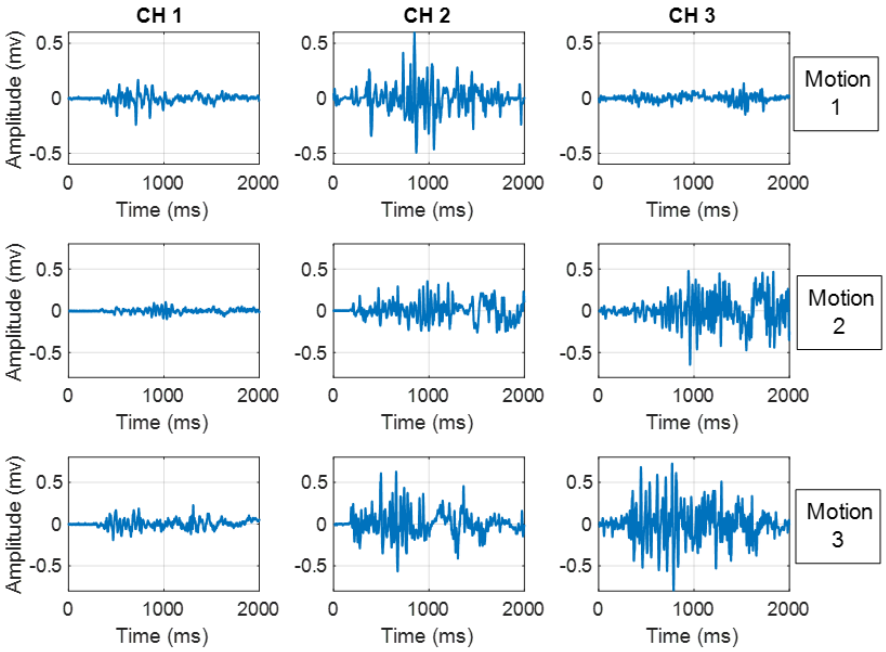

Figure 3-1 Sample electromyography (EMG) signals for different motion.

Figure 3-1 displays three channels and raw EMG signals matrix captured for 2 seconds. From the figure, motion 1 produces a higher EMG signal on Ch1 (column 1) and Ch2 (column 2) compared to Ch 3 (column 3). The second row describes the results of motion 2, the muscles that are most active to produce the EMG signal voltage are the anterior deltoid (Ch3) and bicep brachii (Ch2) muscles, while the brachioradialis muscles tend to produce minimal tension. Meanwhile, motion 3 is seen in the third line, where all channels appear to generate EMG signal activity.

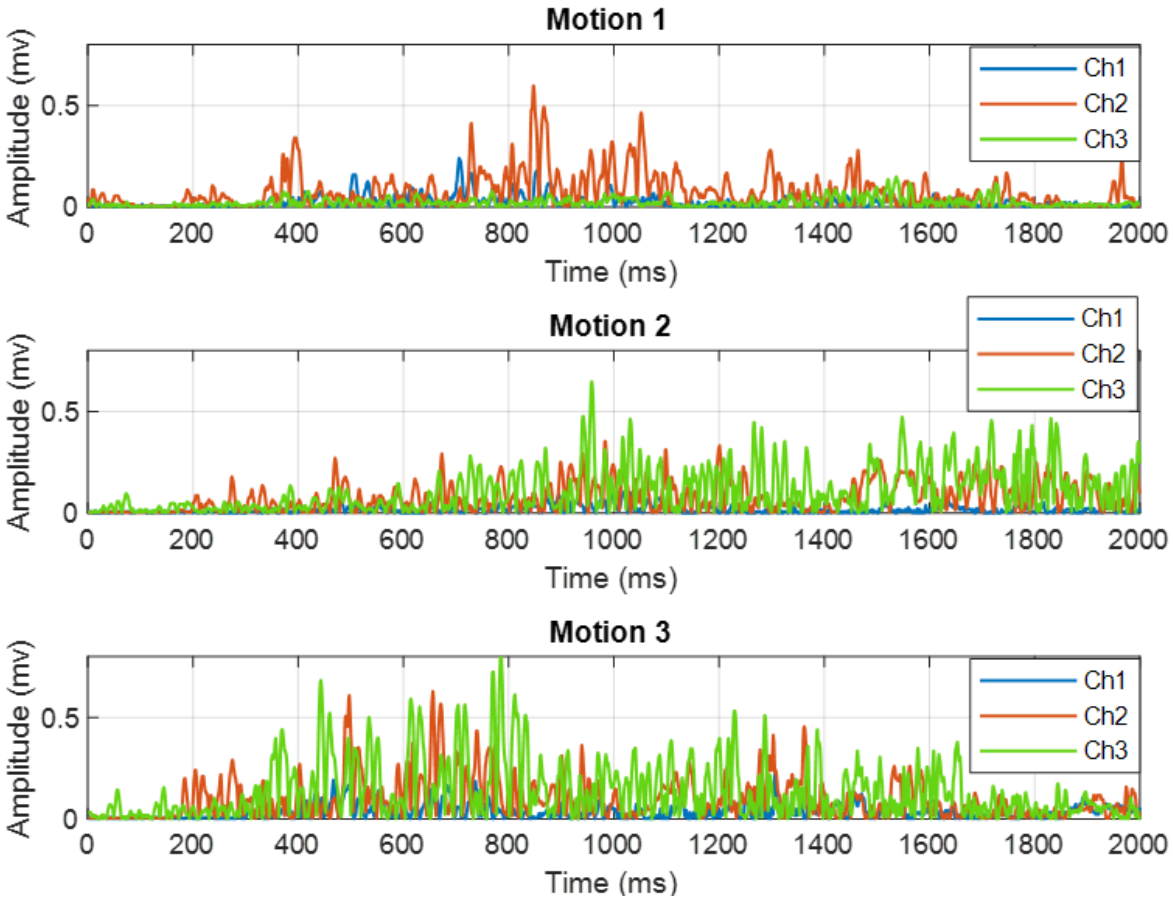

Figure 3-2 Rectified EMG signals.

Figure 3-2 displays the result of EMG after rectification. Rectification basically yields the magnitude of the signal without its polarity. The full-wave rectified results show oscillatory input of the muscles from the neural activation that EMG signals. This is inherent in all EMG signals, and hence, further processing is necessary to ensure usability. Further processing is performed to arrive at a processed signal.

The results of the normalized and processed signal are reported in figure 3-3. From the figure, the onset of raising hand motion is clearly discernable as well as lowering motion. From the design of the experiment, 2 seconds was found sufficient to capture all the motion. Motion 3 had the strictest time budget, while motion 1 had excess time that resulted in the capturing of motion not related to the research. This excess motion

included wrist flex, as will be discussed later.

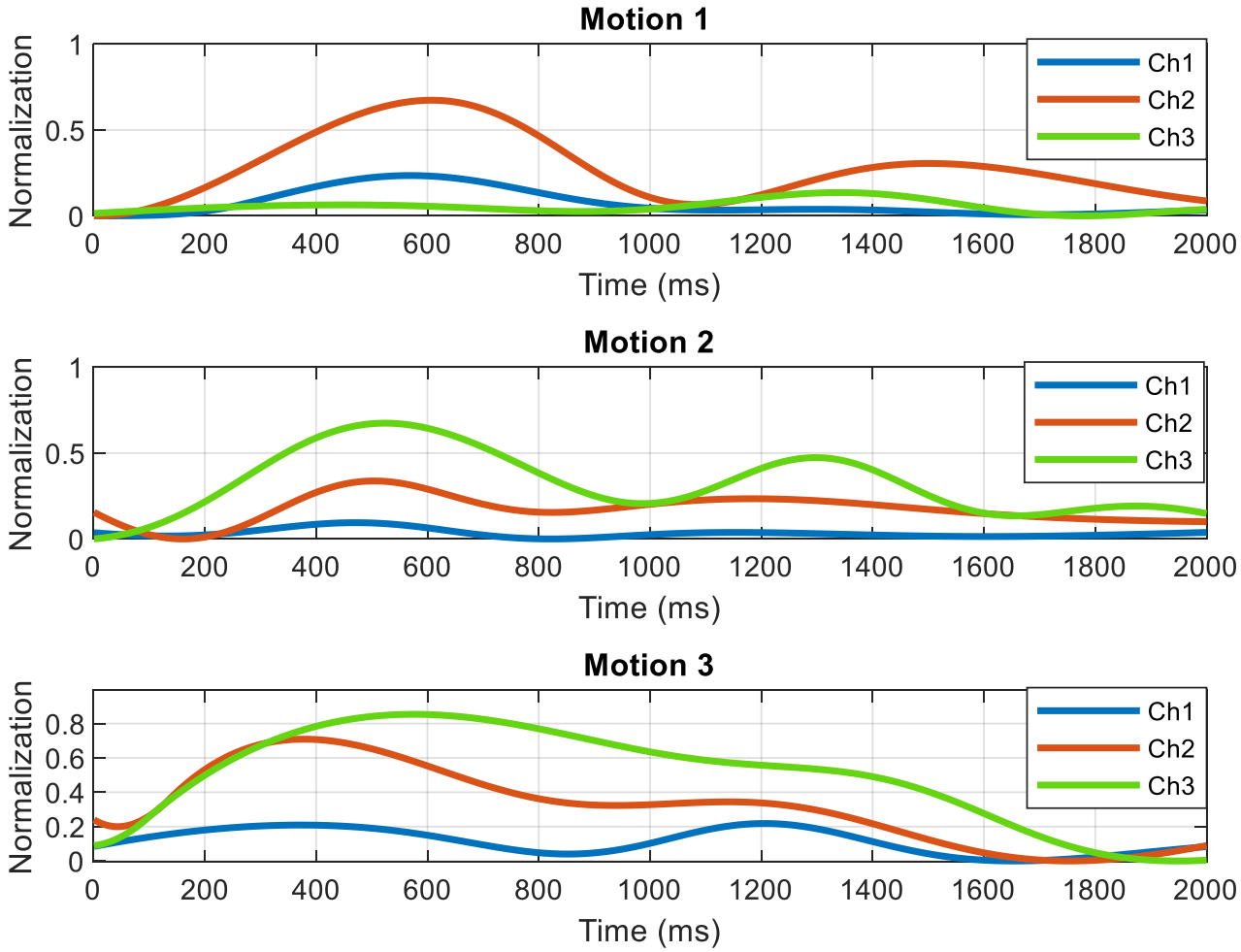

Figure 3-3 Normalized processed EMG signals.

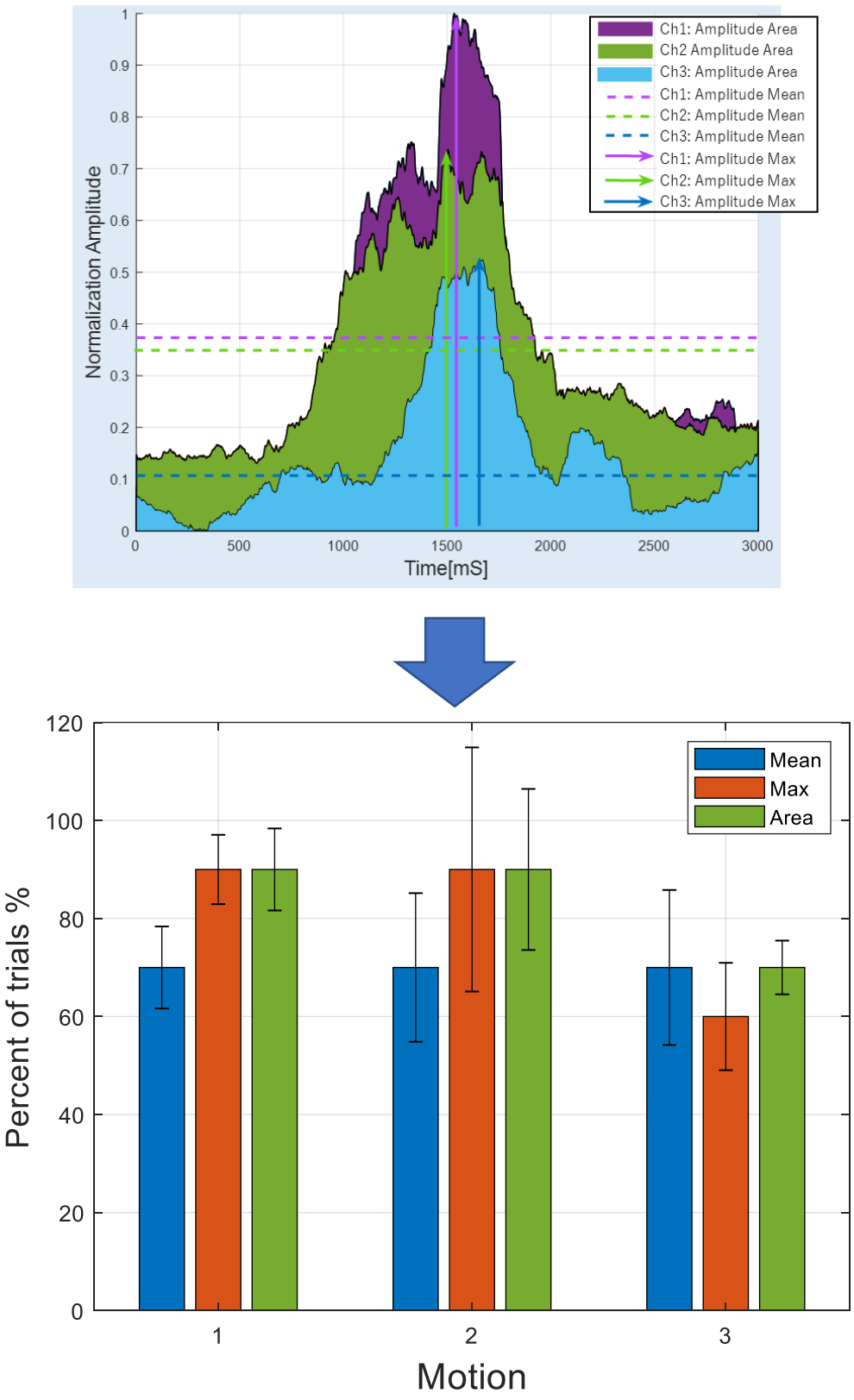

Figure 3-4 Comparizon on 3 Feature Extraction Methods for 3 iEMG Amplitudes.

Figure 3-4 reports the comparison of three control parameters; mean of the envelope (shown as Mean in the figure), maximum amplitude (Max), and area under the curve (AUC) of the envelope signal (Area). From the results, the AUC of the signal displays more consistency in the accuracy of successful control for each motion better than the Mean and Max methods. Besides the comparison of accuracy, the consistency of the results for different motions was an important factor to consider in choosing the model for the robot arm control. It can be seen in figure 3-4 that the area shows the highest level of accuracy compared to other parameters for each movement. Also, the consistency, calculated as average error for each control parameter, was least in the AUC method. The average error of AUC was 10.1% compared to the Mean and Max methods that reported an error of 13.1% and 14.3%, respectively. From this, AUC parameter is maintained in the rest of the document for inter-subject evaluation of performance.

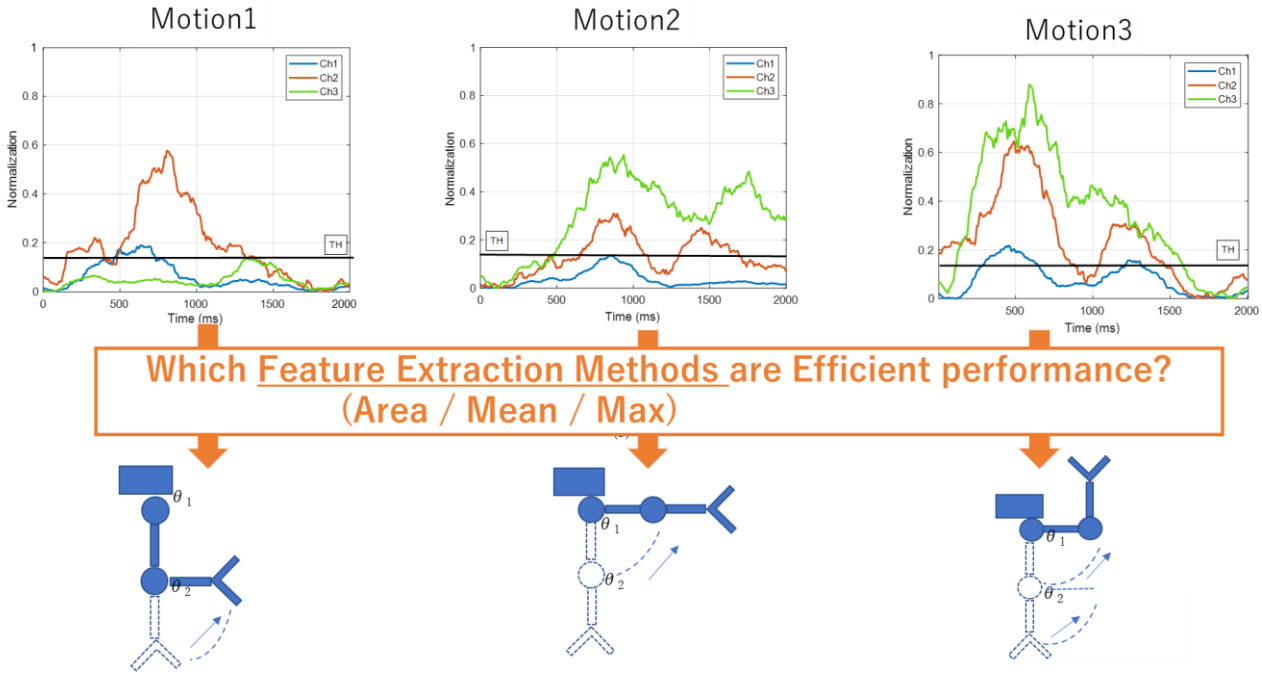

Figure 3-5 Upper pictures for subfigure (a),(b), and (c) are shown each robot arm motions, besides lower pictures show discrimination of the EMG signal motion 1, motion 2, and motion 3 respectively.

(c)

Figure 3-5 illustrates the robotic arm motion corresponding to the discriminated motion. From Figure 3-5(a), which corresponds to Motion 1, brachioradialis muscle (CH1) and biceps brachii (CH2) surpass the baseline threshold. In figure 3-5(b) for motion 2, CH2 and CH3 surpass the threshold, with CH2 being more dominant. In motion 3, all the channels surpass the threshold. From this, it can be seen that anterior deltoid muscle (CH3) plays a major role in motion 2 and motion 3. Biceps brachii (CH2) is equally significant in motion 2 and 3 but more pronounced in motion 3. This can be understood intuitively by the extended nature of motion 2, compared to the clenched elbow joint in motion 3. A visualization of motion and corresponding robot manipulation can be found in this link: https://rb.gy/lfq1iv. The video illustrates controlling a robotic arm using EMG signals in an offline system.

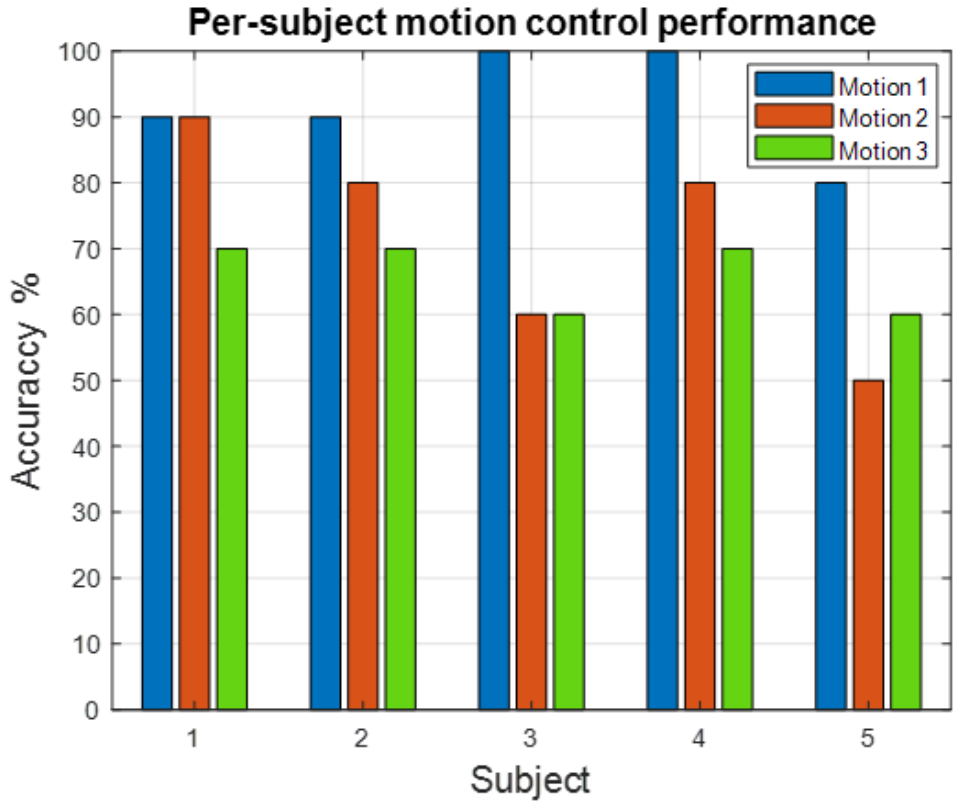

Figure 3-6 Percentage of successful control of the robot arm.

The results of the comparison of intersubject performance carried out in the experiments are shown in figure 3-6. It reports the accuracy of the output of successful robot control out of the repetition for the five subjects. Subject 1 have an overall accuracy : 83.3%, subject 2 :80%, subject 3,4 and 5 are 73.3%, 83.3% and 63.3% respectively. Motion 1 get highest accuracy 100%,beside motion 2 get lowest 50%. Subject 5 had the lowest accuracy at 63.3%.

This was attributed to inconsistent muscle activity during recording. Muscle inconsistency resulted from excessive force employed during motion that is not part of the target muscle activity. This included wrist motions (fist crunching, flexing, or rotations), among others. The discrepancy in the muscle activation introduced difficulty in proper threshold determination. Additionally, we noted timing errors in motion 3 to be a challenge for the two subjects. Besides the motion artifacts, noise and other crosstalk artifacts affected the quality of the signal and thereby affected the prediction of intention from the signal, which is expected from EMG processing [1], [26], [43]. This presented as overshoots and oversaturation in the amplification gain whenever the users overexerted the motions. This was remedied by familiarization repetitions and feedback from the experimenter during preparatory steps.

From the above, the implementation of upper arm control using the two main joints of the elbow and shoulder is possible. The EMG signal obtained from the movement of the upper arm can be observed and the movement mapped. Based on Farina et al. [47], there are several criteria for implementing ideal prosthetic arm such accuracy, intuitively, robustness, adaptive for the user, the minimum number of electrodes, short and easy training/calibration, feedback on relevant functions/close loop control, limited

computational complexity, low consumptions, response time. There is no ideal system to date that meets all of the criteria, but several researchers have tried at least some of these criteria. In this research, we have attempted to optimize target muscle and characterize the upper-limb motion for 2D robot control. The challenge with the approach is a priori knowledge of the sensor data required to inform the choice of threshold. An adaptive threshold determination algorithm and pattern recognition will be explored to further the research. Overall, the development of a measurement control system that improves accuracy, robustness, response time can be attained from this control scheme.

This research presented an EMG investigation of the upper-limb motion-based interface for human-robot interaction in terms of teleoperation tasks. This research demonstrates that three EMG signals that correspond with upper-limb motions have been discriminated and applied successfully for controlling the robotic arm. The area under the curve parameter control yielded more consistency in performance better than the mean and maximum amplitude signals of parameter control. Based on the model's discrimination that generated from the EMG signals envelope using moving average processing signal, the result shows that models can be used for all subjects to control the robotic arm for conducting single and two DOF movements with its simplicity and low computation cost. Also, the performance of the systems statistically describes the accuracy of all motion for all subjects that varies from 50% to 100%. Subject 1 have an overall accuracy : 83.3%, subject 2 :80%, subject 3,4 and 5 are 73.3%, 83.3% and 63.3% respectively. Motion 1 get highest accuracy 100%,beside motion 2 get lowest 50%. Subject 5 had the lowest accuracy at 63.3%. Further developments will include an improved control scheme using pattern recognition, and better methods can be used to tackle the limitation of the system.

Chapter 4 Minimum Mapping from EMG Signals for Controlling Two DoF Upper-Limb Robot using Machine Learning

4.1 Background

Electromyography (EMG) has been considered an important area for study, especially as biological signal control to promote quality of life and self-reliance. There are several areas of applications of EMG, such as disease diagnosis, rehabilitation evaluation, and control strategy for the assistive device. EMG provides rich information obtained by muscle contractions [1], [3], [5], [8], [23], [24], [47]–[49]. Recent research developments in the field of robots have led to robotic arm control with very complex mechanical capabilities, sensor technology, and control algorithms that do not necessarily make it easier for users to intuitively control robots [1], [24], [26], [47]. Hand gesture recognition (HGR) is an important part of human–robot interaction that studies to recognize commands from humans by the development of robot technology. HGR models are human–computer systems that predict what motions or gestures were conducted and when a human conducted the gesture [1], [8], [23], [24], [26], [49]. Human–robot interactions (HRI) are a wide research field. Currently, those systems are used in many applications and researches such as robot control systems [11–23], medical recognitions and rehabilitations [6], [60]–[62], and intelligence assistive devices [8], [11], [17], [36], [54], [63]–[67].

There are several issues related to the process of controlling the robotic arm using the EMG signal. Noise, motion artifact, and crosstalk have an impact on the

prediction intention. The high variability of EMG signal amplitude estimation is a challenge in developing the control system [3,23,35–38]. Ideally, an assistive upper limb robotic arm system should fulfill several criteria such as an intuitive interface for the user; robust system; adaptive to the user; minimal number of sensors and not sensitive to the precise muscle placement; short and easy training/calibration (possibly without training); provide feedback (closed-loop control); low cost and simple computational; and produce good estimation with perceivable delays (real-time) [4,8,14,25,29,39]. Laksono et al. [3] proposed a model mapping for three EMG channels from three different muscles to control the robotic arm to predict three movements of the upper arm. This simple model can discriminate against three upper arm movements by considering the influence of the targeted muscle position when doing the movement; the characteristics of the muscles that perform the activity will play an important role in carrying out the movement. Even though the model was capable of performing motion mapping, the overall reported accuracy in 76.64% was still not optimal. The existing research on the classification of hand movements based on EMG signals still faces many challenges such as weak robustness, the minimum number of sensors, short training data, low computational process, and good prediction with perceivable time delay [2,4,10,34,39–43]. To address these challenges, we propose models for classifying upper arm movements that conducted 1- and 2-degrees of freedom (DoF) motions using machine learning. The HGRs include three movements (elbow extension, shoulder extension, combined shoulder and elbow extension), and a case with no movement (default condition). Simultaneous and independent control of multi degrees of freedom (DoF), such as elbow and shoulder joints, is the main target of the machine learning-based model for controlling robotic arm using electromyography (EMG) signal [18]. This research also focused on the positioning of

the EMG sensor on the target muscles that are directly involved in the movement of the upper arm. In this research, we introduce machine-learning models for controlling the robot arm that EMG signals are obtained from three muscles as a multi-channel (three channels of input). This three-motion produced four class predictions consist of motion 1, motion 2, motion 3, and no motion.

Machine learning has been used extensively in HGR and other EMG-related studies targeting different functionalities. Several kinds of research focusing particularly on elbow and shoulder movements have been reported in Triwiyanto et al. [45], Antuvan et al. [55], Martinez et al. [56], Hassan, Abou-Loukh, and Ibraheem [28], Young et al. [77], Jiang et al. [46], and Tsai et al. [47], classification of upper limb motion using extreme learning machines by Antuvan et al. [74], using Support Vector Machine (SVM) [6,8,19,48], investigation of shoulder muscle activation pattern recognition using machine learning by Jiang et al. [78], and detection movements using EMG signal for upper limb exoskeletons in reaching tasks by Trigili et al. [80]. These papers verify the suitability of EMG signals for biopotential intelligent robot control.

The key to any EMG control is the measurement system in use. As expected, accurate EMG signal recording increases the performance of the pattern recognizing model. In this paper, the experiment was conducted systematically to investigate the impact of using Teager–Kaiser energy operator (TKEO) and variable segmentation levels of EMG signal input. To get better classification performance and try to tackle the challenges, we propose the following framework to classify EMG signals for controlling a robotic arm. The use of multi-channels for data retrieval has aided in recognition as it covers more muscle areas. Hence, in this research the focus of EMG data collection is in

three positions, namely brachioradialis, biceps brachii, and deltoid to move the robotic arm. EMG processes such as data segmentation had similarly been shown to better the results of discriminative models[67]. We performed three levels of data segmentation. On the first level, no segmentation was performed. On the second and third level, the EMG signal was split into two or three segments of data and treated as distinct input to feature extraction process. To overcome muscle activation signals, TKEO was used for onset detection[79], [81], [82]. TKEO method has been mainly used to enhance the magnitude and frequency of time-domain signals without requiring the conversion of those signals to the frequency domain [41]. The other preprocessing processes, such as normalization, rectification, and smoothing signals using moving average, are commonly used by many researchers [29], [30], [79], [83].

Feature extractions take an important role in machine learning. Features were extracted from the different EMG signal sources. The feature of EMG signals commonly includes time-domain (TD) and frequency-domain (FD) feature. Feature extraction proposed in this paper was multi-feature TD, which includes the mean absolute value (MAV), zero crossings (ZC), slope-sign changes (SSC), and waveform length (WL) [29], [79], [83]–[85]. A calibration phase was utilized to acquire training phase data. From this, we evaluated the features as well as extent of the sampled data. In total, four classes (motion 1, motion 2, motion 3, and no motion) were classified. Machine learning model classifiers were used as a feasible decoder to predict the four movements. The results obtained in this study were applied online for real-time implementation. The performance shown includes a fairly accurate and consistent prediction accuracy. Three metric performances; accuracy, recall, and precision were evaluated for evaluation of performance. In real-time processing, there were various optimal controller delays in the

literature review that reported below 500 ms which is still feasible for real-time robotic control [23], [24].

In this paper, we deployed a teleoperation HRI cooperating between surface EMG and an upper-arm robotic, to fast-detect the user's hand gesture intention. We implemented an offline supervised machine-learning algorithm, using a set of five subject-independents. The proposed system established various scenarios consisting of three-level variables of segmentation signal, using TKEO, and classification types of the machine-learning model, such as decision tree, k-Nearest Neighbor (KNN), SVM, and Ensemble. All machine-learning algorithms are provided in the classification learner application in Matlab®. The significant contribution of this study is to provide the results of investigations regarding the optimal performance of the supervised machine-learning model using limited data training to classify upper arm motions based on three EMG signal channel inputs from three different target muscles and to control the robotic arm in teleoperation HRI simultaneous.

4.2 Experiment

Five healthy subjects participated as volunteers for the experiment. All of the participants provided written informed consent letters following approval procedures (number 27–226) issued by the Gifu University ethics committee and complying with the Helsinki declaration. This experiment explored machine-learning approaches that can be useful in the prediction of elbow and shoulder joint movements classification as an alternative to the modeled equation for robotic controlling. The proposed experiment system used to describe the process of controlling the robotic arm using EMG signal classification is illustrated in figure 4-1. The subjects conducted upper limb motion which

was similar to our previous research. The experimental setup that included EMG measurements system, muscle position, data acquisition, data analysis, and robotic control is described by Laksono et al. [3].

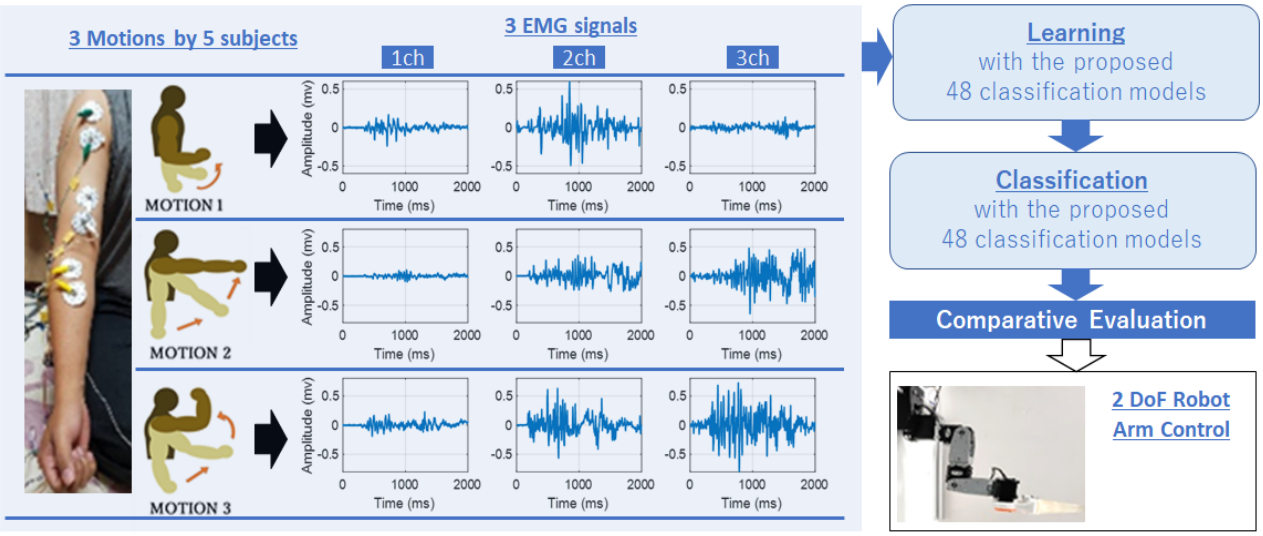

Figure 4-1 The proposed system for electromyography (EMG) controlled robotic arm.

4.2.1 Feature Extraction Stage

EMG signals are easily corrupted by the environment in the data acquisition process. Motions artifacts, crosstalk, baseline offset, and power line frequency may lead to distortion in the process classification [41,48,52,54,56,57]. We used an isolator to reduce the powerline frequency noise. Three EMG sensors were used to capture EMG signals and then they were used as inputs for the learning process. Teager–Kaiser energy operator (TKEO) was used for enhancing the amplitude and frequency of TD EMG signals without converting those signals to the FD [41–43]. TKEO was performed to enhance muscle activation detection. The TKEO is denoted in Equation (14):

$$\gamma[x(i)] = x^2(i) - x(i+1) \times (i-1) \tag{14}$$

Then, the conventional EMG feature extraction methods were employed to extract meaningful information for EMG signal classification. Each of them is explained below.

Mean absolute value (MAV) was used as an onset index to detect muscle activity. MAV is the average absolute value of EMG signal amplitude. MAV is a popular feature used in EMG hand movement recognition applications [85]. It is defined as

$$MAV = \frac{1}{M}\sum_{i=1}^{M}|Xi| \tag{15}$$

Waveform length (WL): WL is the cumulative length of the waveform overtime segment. WL is similar to waveform amplitude, frequency, and time [85]. The WL can be formulated as

$$WL = \sum_{i=1}^{M-1}|Xi+1-Xi| \tag{16}$$

Zero crossing (ZC) is the number of times that the amplitude values of EMG signal cross zero in the x-axis. In the EMG feature, the threshold condition is used to

avoid background noise. ZC provides an approximate estimation of frequency domain properties [85]. The calculation is defined as

$$ZC = \sum_{n=1}^{N-1} [f(x_n - x_{n+1}) \cap |x_n - x_{n+1}| \geq threshold]$$

$$f(x) = \begin{cases} 1, & if\ x \geq threshold \\ 0, & otherwise \end{cases} \tag{17}$$

Slope-sign change (SSC): SSC is related to ZC. It is another method to represent the frequency domain properties of EMG signal calculated in the time domain. The number of changes between positive and negative slope among three sequential segments is performed with threshold function for avoiding background noise in EMG signal [85]. It is given by

$$SSC = \sum_{n=2}^{N-1} \left[f[(x_n - x_{n-1}) \times (x_n - x_{n+1})] \right]$$

$$f(x) = \begin{cases} 1, & if\ x \geq threshold \\ 0, & otherwise \end{cases} \tag{18}$$

4.2.2 Machine Learning (ML) Stage

The classification started with preparing data for the learning process. Data was generated from three EMG channels recorded at a sampling rate of 2000 Hz with recording times varying between 1.5–3 s per motion stored in the workspace. In total, five subjects performed three motions. The data were segmented as follows; 60% for training and 40% for performance validation.

As mentioned, 40% of the data was reserved for testing/inferencing. The machine learning models operate as shown in figure 4.2. In this case, the learning algorithm is fed with a pair of training data, which conventionally includes a response signal and a corresponding correct signal, which acts as a teacher. After the learning phase, inferencing can be made with the generated model. This output prediction based on weightings of the learned model for accurate inferencing; the data supplied should be novel to the model and hence the separation into testing data employed in the model.

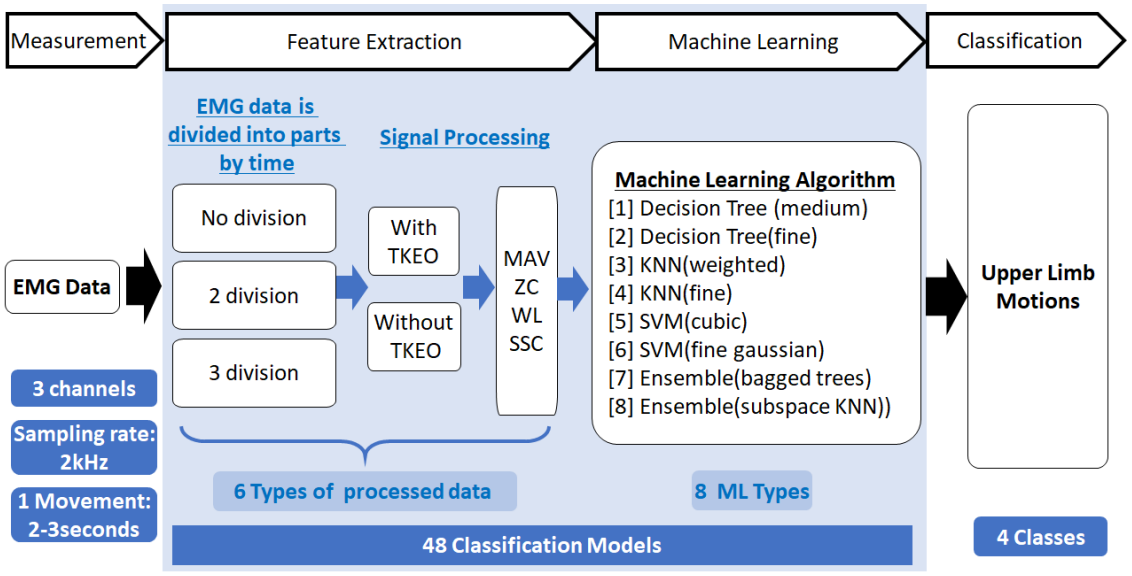

Figure 4-2 Classification models for comparative evaluation.

Figure 4-2 illustrates the proposed machine learning model subdivision (six scenario models) utilized in the systematic investigation of optimal controller. The data is subdivided into two groups; processed with TKEO and without TKEO dataset. For each of the datasets, three variations of data are applied with the variation of dividing the signal into no segment, two segments, and three segments as inputs for training. Feature extraction is performed on each of the models to arrive at a trained model. A total of 48 types of trained models were investigated.

We used four features (MAV, WL, ZC, and SSC as multi-features from each channel) for training in one segment as an input. As such, 13 predictor signals (features) and one correct "teacher" signal were fed to the training model. For the second data input (using two segments input for each channel), we used similar features resulting in 25 predictors. Then, three segments were input in 37 predictors. It is worth noting that the same data was fed to the two distinct groups for comparison purposes. In both cases, we used five-fold cross-validation for accuracy estimation and to avoid overfitting.

A Matlab classification learner application that performs multiclass error-correcting output code with the different learner models was employed. In this case, eight types of machine learning learner models were employed; decision tree (medium), decision tree (fine), KNN (weighted and fine), SVM (cubic and fine Gaussian SVM), Ensemble (bagged trees and subspace KNN) were used. The hyperparameters for each classifier were initialized with the default setting. All ML methods performed training data properly. Based on the prediction performance (see table 4.1), KNN (fine) and ensemble (subspace KNN) algorithms had the best accuracy for the method using TKEO and the method without using TKEO, respectively. These models were used for further analysis, shown in the next section.

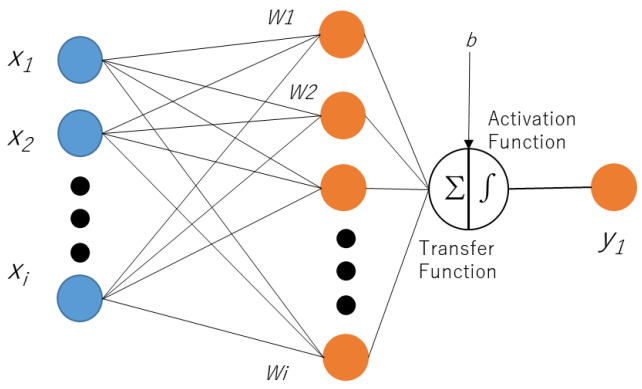

Figure 4-3 Schematic view of neural network for machine learning

In this research, a binary classifier used in supervised learning used to classify a given input data. It comprises of an input, weight, threshold, summer, and an activation function related to which kind of machine learning model used. The neural network model (see figure 4-3) contains three layer (inputs(x_i), a hidden layer, and outputs(y_i)), we proposed multiclass classification model for controlling robotic arm. As each signal is set on matrix, we set three kind of EMG signals input. Three kinds inputs are 13 (3 channel x 1 division x 4 features + 1 correct signals), 25 (3 channel x 2 division x 4 features + 1 correct signals) and 37(3 channel x 3 division x 4 features + 1 correct signals) as input predictors. The hidden layer is activation functions which based on what kind of machine learning model are used such as decision tree (medium), decision tree (fine), KNN (weighted and fine), SVM (cubic and fine Gaussian SVM), and Ensemble (bagged trees and subspace KNN). The outputs are four classes (motion 1, motion 2, motion 3, and no-motion).

Table 4-1 Machine learning type parameter setting

Machine Learning	Chareacteristics	Parameter Settings
Decision Tree (medium tree)	+ Easy to prepare, to read and to interpret. + Less data cleaning required – Small data can be instability	Maximum numbers of splits = 20,
Decision Tree (fine tree)		Split criterion = Gini's diversity index,
KNN (weighted)	+ Quick calculation and prediction + versatile : easy to make prediction – Large and high dimension dataset problem – Sensitive to noise data	Maximum numbers of splits = 100;
KNN (fine)		Split criterion = Gini's diversity index
SVM (cubic)	+ Works well with unstructured and semi structured data like text, Images	Number of neighbors = 10; Distance metric = Euclidean

SVM (Fine Gaussian)	and trees. +They used kernel for training – finding good kernels parameters are not easy	Distance weight = square inverse;
Ensemble (Bagged Trees	+ Multiple models are used to make prediction	Number of neighbors = 1; Distance metric = Euclidean
Ensemble (Subspace KNN)	+ Reduces generalization error during prediction – slow calculation and prediction	Distance weight = equal;

Decision tree is often used as machine learning methods. The hierarchical structure of a decision tree leads us to the final outcome by traversing through the nodes of the tree. Each node consists of an attribute or feature which is further split into more nodes as we move down the tree. In this study, we used Gini's diversity index (see equation 19) for splitting criterions and maximum number of splits 20 (fine tree) and 100 (medium tree)

$$Gini = 1 - \sum_{i=1}^{n} (p_i)^2 \quad (19)$$

where pi is the probability of an object being classified to a particular class. The degree of Gini index varies between 0 and 1, where 0 denotes that all elements belong to a certain class or if there exists only one class, and 1 denotes that the elements are randomly distributed across various classes.

One of the classifications of machine learning methods with advisory learning is KNN. Under the structure from the training dataset, the classification is carried out according to the nearest distance to points in a training data set. In this study, we used

model type fine KNN with k = 1 selected, and Euclidean distance calculation formulas were used. The choice of the K value to be used varies according to the dataset. As a rule, the fewer neighbors (a small number K) we have, the more we are subject to under-fitting

$$d(x, x') = \sqrt{(X_1 - X'_1)^2 + (X_2 - X'_2)^2 + \cdots + (X_n - X'_n)^2} \qquad (20)$$

SVM has extensively discussed resolution methods for pattern-based classification for control applications. Two different kernels (Cubic and Gaussian) were used to classify four different arm movements, through 3 EMG signal channels, by combining four feature extractions MAV, WL, ZC and, SSC in such a way that in total three kinds of vectors (13,25, and 37) are introduced to SVM. Cubic and gaussian are specified kernel function to compute the matrix. We set kernel scale automatic, box constraint level set 1, multiclass method set one-vs-one and standardize data to improve the fit

Ensemble classifier is a system made by combining different classifiers to produce more safe and stable predictions [86]. The system is built with the N classifier that can be single or multiple, while the classification is appropriate to the feature vector, for each feature vector 1, each classifier yields the output value (the resulting output value is counted). Then, the output of the ensemble classifier is determined by the number of votes. If the number of classifiers is, in fact, the average value of the classifier's decision, it is rounded off, and the ensemble classifier decision is determined. All feature vectors are applied by this process [87]. We used the ensemble (subspace KNN) method using six dimensions subspace and learner nearest neighbors using 30 learners.

4.2.3 Performance Analysis

The performance of six trained models was compared based on classification accuracy. The performance of the ML for each model is shown in table 4.1 below. From the table, accuracy ranged between 80.5% - 98%. The highest accuracy was selected as the target model for evaluation. As such, Ensemble (subspace KNN) was chosen for model 1, 2, 3, and 6 while KNN (fine) was chosen for model 4 and 5.

Table 4-2 Accuracy of machine learning training model prediction performance.

6 Feature Extraction Types		8 Machine Learning Types							
		A	B	C	D	E	F	G	H
		Decision Tree (Medium)	**Decision Tree (Fine)**	**KNN (Weighted)**	**KNN (Fine)**	**SVM (Cubic)**	**SVM (Fine Gaussian)**	**Ensemble (Bagged Trees)**	**Ensemble (Subspace KNN)**
	a	80.5%	80.5%	89%	89%	89%	82%	84.5%	92.5% (6)
	b	74.5%	74.5%	92%	95.5%	92%	75.5%	89.5%	96% (4)
	c	77%	77%	93.5%	94%	93%	74%	86%	95% (5)
	d	90%	90%	94.5%	96.5% (2)	95%	95.5%	91.5%	96%
	e	82%	82%	93%	96.5% (3)	93.5%	92%	90%	96%
	f	85%	85%	93.5%	97.5%	95.5%	94%	93.5%	98% (1)

The confusion matrix for five subjects is plotted in fig. 4-4, fig. 4-5, and fig. 4-6. From the figures, all models achieved significant performance with regard to accuracy. Motion prediction comparison shows that the rank of accuracy class 2 (motion 2) is higher than the others, and class 3 (motion 3) is the lowest rank. The best accuracy is having a bigger number of true-positive rates (TPR) than others and a smaller number of false-negative rates (FNR). Mostly all training models have the value of TPR about 74%–96.5% and the value of FNR about 0–16%. Compared with 65 primary studies reviewed by Jaramillo-Yanez et al. regarding the use of ML on HGR using the EMG signal, the

accuracy of the classification model resulted in a range of 70–100% [23]. We showed that all ML training models are working and predicting properly.

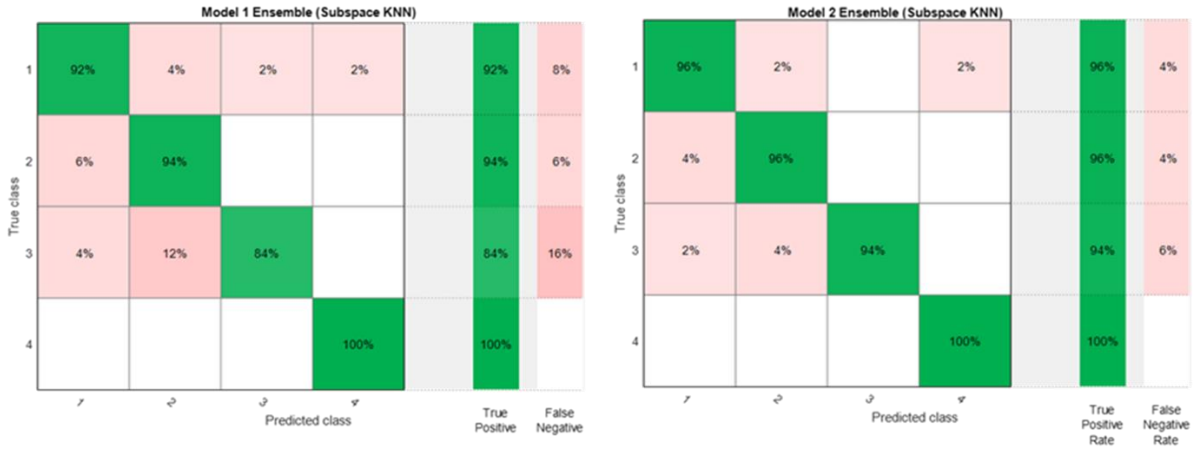

Figure 4-4 Confusion matrix of discrimination model 1(left) and model 2 (right).

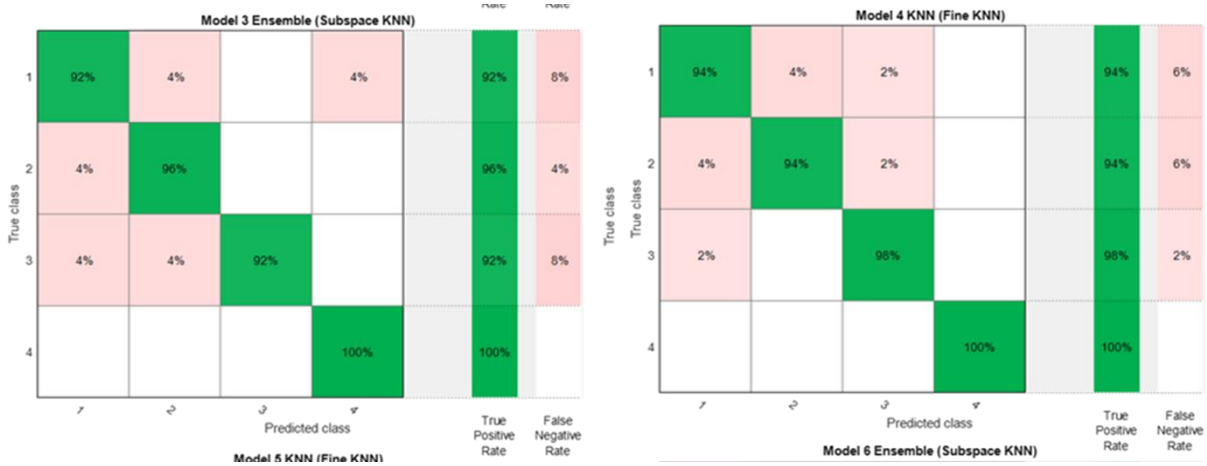

Figure 4-5 Confusion matrix of discrimination model 3 (left) and model 4 (right).

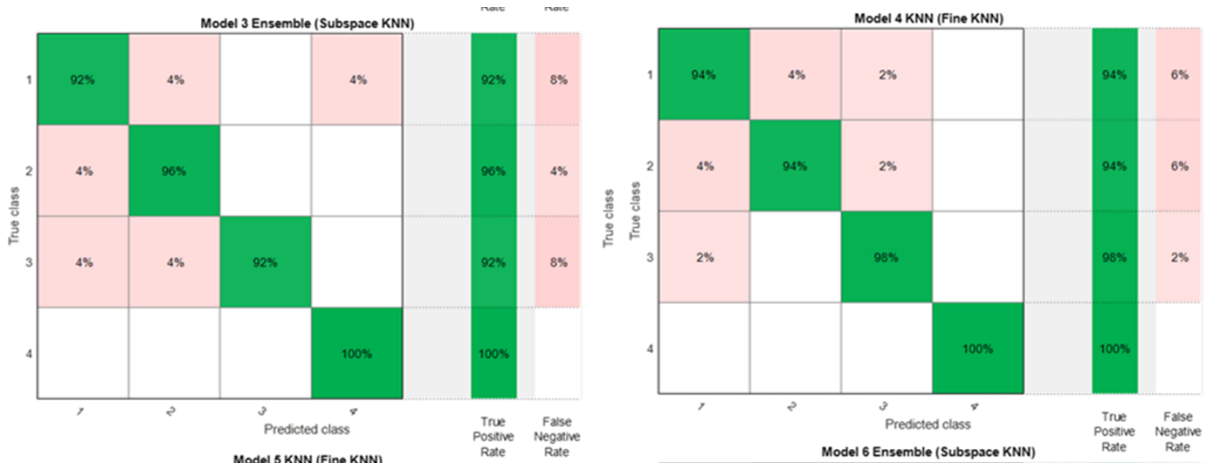

Figure 4-6 Confusion matrix of discrimination model 5 (left) and model 6 (right).

The prediction performances in every motion were computationally analyzed using three performance metrics: accuracy, recall, and precision. The classification accuracy metric (see equation 21) is the ratio of motions perceived correctly among all of the test data. The classification recall metric (equation 22) is the fraction of motions predicted correctly for a class among the test data of this class. The precision metric (Equation 23) is the ratio of motion realized correctly from a class among the motions recognized by the ML model as this class [23].

$$Accuracy_{user(i)} = \frac{\sum_{j,k=1}^{g} n_{i,j,k}}{\sum_{j=1}^{g}\sum_{k=1}^{g} n_{i,j,k}} \quad 21)$$

$$Recall_{user(i)class(k)} = \frac{n_{i,k,k}}{\sum_{j=1}^{g} n_{i,j,k}} \quad 22)$$

$$Precision_{user(i)class(j)} = \frac{n_{i,j,j}}{\sum_{k=1}^{g} n_{i,j,k}} \quad 23)$$

where $n_{i,j,k}$ is the number of motions conducted by the subject i, which were recognized by the model as j, but they were k. $i \epsilon \mathrm{I} = i_1, i_2, ..., i_u$ is the set of test subjects, $j \epsilon J = j_1, j_2, ..., j_g$ is the set of predicted classes, $k \epsilon K = k_1, k_2, ..., k_g$ is the set of actual classes, u is the total number of test subjects, and g is the number of classes.

4.3 Result and Discussion

Identifying multiple hand motions using a few EMG sensors and muscles is one of the challenges for improving high levels of usability in controlling robotic hands, which we are attempting to solve. The experiment was conducted systematically, and the results are shown below.

The overall performance comparison for five subjects shows that the users could achieve the acceptable percentage of performances, including accuracy (figure 4.5), recall (figure 4.6), and precision rates (figure 4.7). The development of a machine learning model that is used to discriminate EMG signals from three sensor inputs of three muscles for three kinds of movements shows promising results. Scenarios of six models were used based on the level of the frequency cut-out factor in the segmentation, whether or not using TKEO is used, and the model classification. The results of the classifications performance percentage of the five subjects are, for the accuracy rate, in the range of 65%–100%, for the recall rate, in the range 91%–100%, while for the precision rate, in the range of 70%–100%.

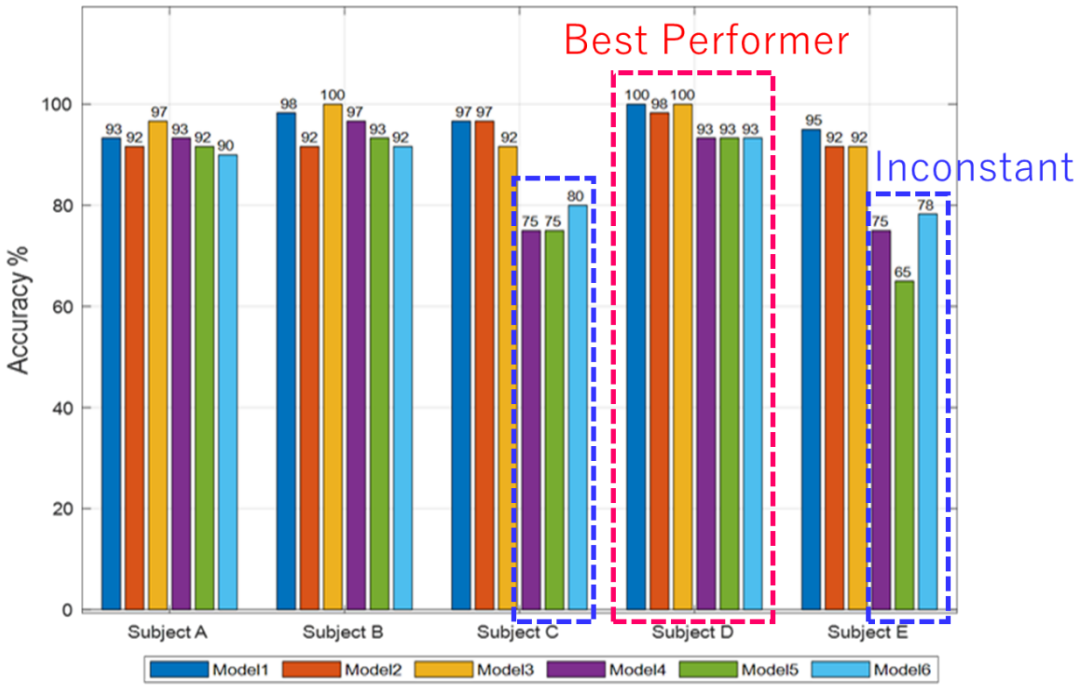

Figure 4-7 Average classification accuracy percentages per 5 subjects.

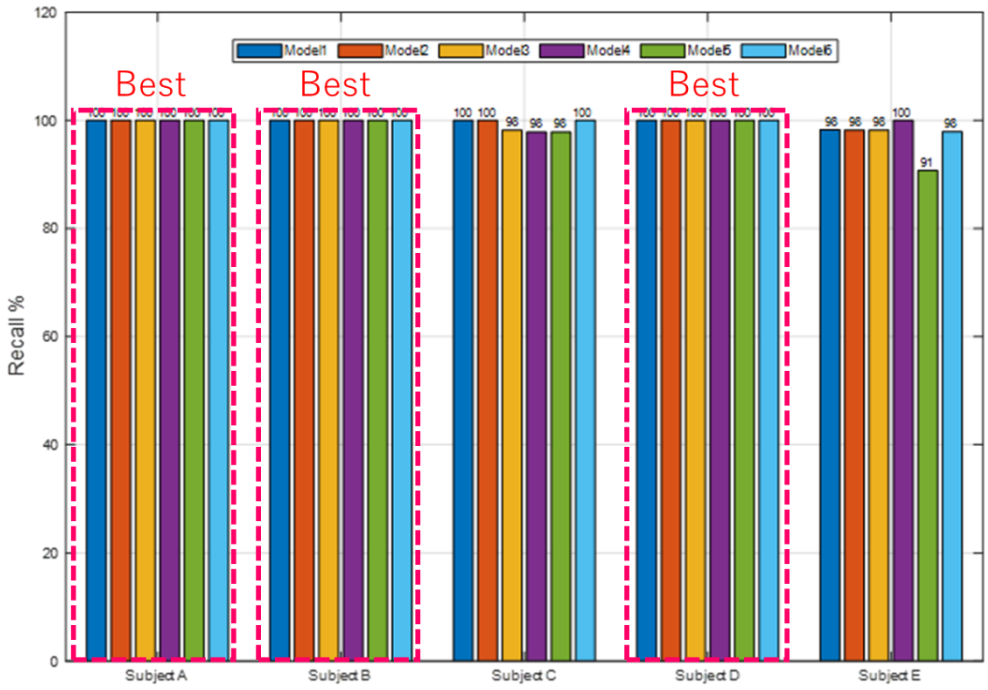

Figure 4-8 Average classification recall percentages per 5 subjects.

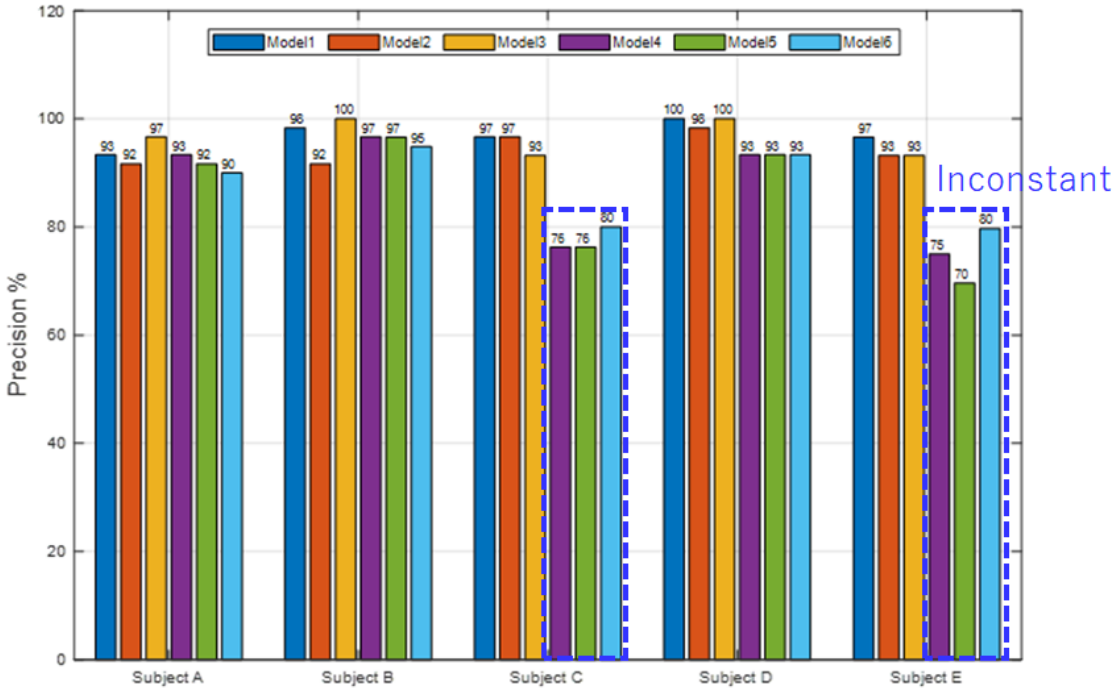

Figure 4-9 Average precision percentages per 5 subjects.

Table 4-3 Total performance index

Model	Accuracy	Recall	Precision
1	96.67%	99.66%	96.99%
2	94%	99.64%	94.31%
3	96%	99.29%	96.62%
4	86.67%	99.57%	86.92%
5	83.67%	97.7%	85.49%
6	86.33%	96.97%	89.31%

Subject D reports the highest consistent accuracy results than the others, model 1 achieved the highest average percentages of accuracy at 97.67%, while model 6 obtained the lowest at 86.33 %(see table 4.3). At least all the subjects reported consistent results for recall rate, ranging from 96.97% to 99.67%. Subject A had the most consistent precision with model 1 which reported an average precision of 96.99%. The reasons why the performances are varied are because of motion artifacts and inconsistent motion issues.

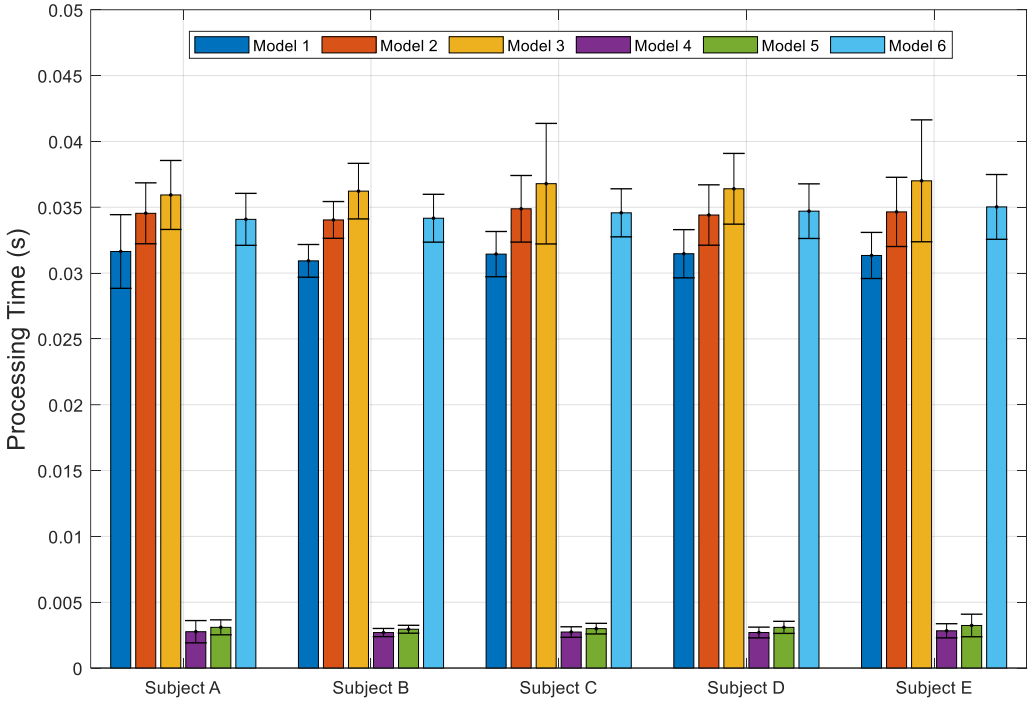

Figure 4-10 Average processing speed time per 5 subjects.

Table 4-4 Average processing speed time of six models.

Model	Average Time (s)	SD
1	0.0314	0.0019
2	0.0345	0.0022
3	0.0365	0.0033
4	0.0027	0.0005
5	0.0031	0.0005
6	0.0020	0.0020

Table 4.3 reports the processing time required for the different ML model classification. The measured delay controller for the HGR model must reach optimal timing. Overall, all the models that are used by the five subjects require less than 40 ms for processing speeds of time data analysis (see figure 4.8). The fastest average processing time is obtained by model 4 at 2.7 ms, while the longest time is acquired by model 3 at 36.5 ms (see table 3). If the data collection time is less than 200 ms and the data analysis

time is added, the embedded system should be quite relevant to categorize as the real-time system[26], [44], [57], [88].

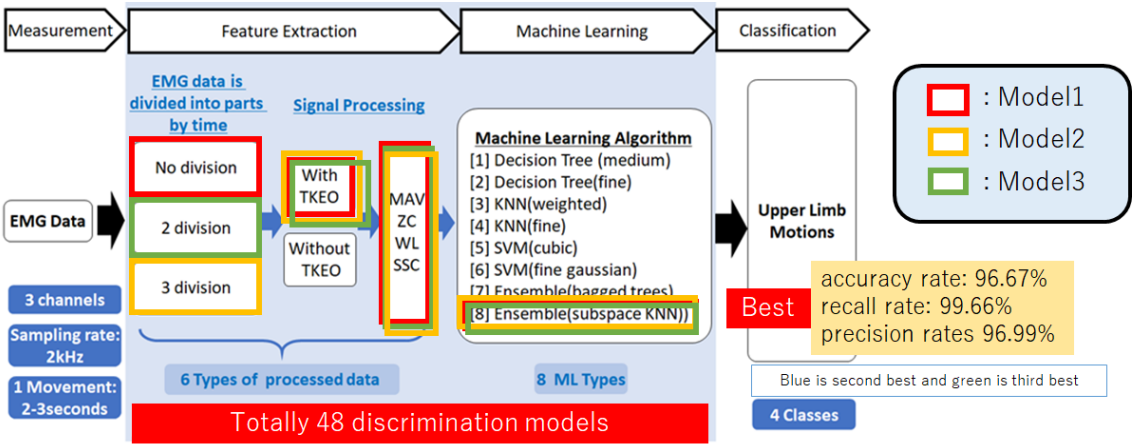

Figure 4-11 Processing flow of 3 Best Discrimination Models.

Based on the performance accuracy rates, recall rates, precision rates, and processing time, model 1 (TKEO processing with no division inputs per channel using ensemble subspace KNN) classification achieved the best performance. Model 1 hit accuracy rates in 96.67%, recall rates 99.66%, and precision rates 96.99%, while model 5 (without using TKEO, two segments input per channel, and four features with ensemble (subspace KNN) classifier)) had the worst performance. Model 5 had performance accuracy rates, recall rates, and precision rates of 86.33%, 96.97%, and 89.31%. Subject D showed more consistent performance than others. Based on this study, using TKEO achieved better performance results. However, inconsistent motions and motion artifacts are the main issue. Improving experiment setup for participants, such as giving a proper explanation and monitoring of participants, can be done to decrease inconsistency.

Chapter 5 Conclusion

In conclusion, the validity of the usage of biopotential signals in robot control has been verified. Three EMG signals generated from three EMG sensors that are mounted at three different muscles that correspond with three upper-limb motions have been discriminated and applied successfully for controlling the robotic arm. Based on the model's discrimination generated from the EMG signals envelope using moving average processing signal, the result shows that models can be used for all subjects to control the robotic arm for conducting single and two DOF movements with its simplicity and low computation cost. The control scheme in use proofed to be manageable with an accuracy range between 50% to 100%. The percentage of accuracy rate per subject ranged 63.3%-83.33%. The highest performance was motion 1 at 100% while the worst performance was motion 2 at 50%.

We designed 48 classification models for discriminating three EMG signals at three upper limb motions and compared and evaluated the minimum parameters of feature extractions and machine learning models with five healthy subjects' data. The results showed that all the proposed models achieved accuracy rates in the range of 74%–98% and the processing speed was below 40 ms, which is an acceptable delay for controlling a robotic arm. Then, the best classification model was discriminated with 12-parameter-ensemble (subspace KNN) accuracy rates of 96.67, recall rates of 99.66, and precision rates of 96.99. The difference between the best model and the conventional model was TKEO. It seemed that TKEO functioned to make the results of MAV, ZC, SSC, and WL stand out. Further research will deal with classifying more than three upper motions with three EMG sensors.

The majority of real-time controlling systems for the robotic arm are still using EMG signals, especially multiple channels targeting multiple muscles to generate multiple synchronous control signals. This should be an open space for investigating in the future for real-time scenarios. Furthermore, to achieve real-time usability, appropriate design of the assistive device, automation of training, data acquisition process, feature extraction, adaptive and robust model, and classification techniques should be properly investigated and implemented.

Reference

[1] A. G. Feleke, L. Bi, and C. Guan, "A review on EMG-based motor intention prediction of continuous human upper limb motion for human-robot collaboration," *Biomed. Signal Process. Control*, vol. 51, pp. 1–17, 2019, doi: 10.1016/j.bspc.2019.02.011.

[2] L. Bodenhagen, S. D. Suvei, W. K. Juel, E. Brander, and N. Krüger, "Robot technology for future welfare: meeting upcoming societal challenges – an outlook with offset in the development in Scandinavia," *Health Technol. (Berl).*, vol. 9, no. 3, pp. 197–218, 2019, doi: 10.1007/s12553-019-00302-x.

[3] P. W. Laksono *et al.*, "Mapping Three Electromyography Signals Generated by Human Elbow and Shoulder Movements to Two Degree of Freedom Upper-Limb Robot Control," *Robotics*, vol. 9, no. 4, p. 83, 2020, doi: https://doi.org/10.3390/robotics9040083.

[4] M. Javaid, A. Haleem, R. Vaishya, S. Bahl, R. Suman, and A. Vaish, "Industry 4.0 technologies and their applications in fighting COVID-19 pandemic," *Diabetes Metab. Syndr. Clin. Res. Rev.*, vol. 14, no. 4, pp. 419–422, 2020, doi: https://doi.org/10.1016/j.dsx.2020.04.032.

[5] M. Sasaki *et al.*, "Robot control systems using bio-potential signals Robot Control Systems Using Bio-Potential Signals," in *The 5th International Conference on Industrial, Mechanical Electrical, and Chemical Engineering 2019 (ICIMECE 2019)*, 2020, vol. 020008, no. April.

[6] L. Bonfati, M. La, and B. Freitas, "Sensors and Systems for Physical Rehabilitation and Health Monitoring—A Review," no. July, 2020, doi: 10.3390/s20154063.

[7] H. Dai, S. Song, C. Hu, B. Sun, and Z. Lin, “A Novel 6-D Tracking Method by Fusion of 5-D Magnetic Tracking and 3-D Inertial Sensing,” *IEEE Sens. J.*, vol. 18, no. 23, pp. 9640–9648, 2018, doi: 10.1109/JSEN.2018.2872650.

[8] R. Meattini, S. Benatti, U. Scarcia, D. De Gregorio, L. Benini, and C. Melchiorri, “An sEMG-Based Human-Robot Interface for Robotic Hands Using Machine Learning and Synergies,” *IEEE Trans. Components, Packag. Manuf. Technol.*, 2018, doi: 10.1109/TCPMT.2018.2799987.

[9] X. V. Wang, Z. Kemény, J. Váncza, and L. Wang, “Human–robot collaborative assembly in cyber-physical production: Classification framework and implementation,” *CIRP Ann. - Manuf. Technol.*, vol. 66, no. 1, pp. 5–8, 2017, doi: 10.1016/j.cirp.2017.04.101.

[10] A. Cherubini, R. Passama, A. Crosnier, A. Lasnier, and P. Fraisse, “Collaborative manufacturing with physical human-robot interaction,” *Robot. Comput. Integr. Manuf.*, vol. 40, pp. 1–13, 2016, doi: 10.1016/j.rcim.2015.12.007.

[11] O. Fukuda, T. Tsuji, M. Kaneko, and A. Otsuka, “A human-assisting manipulator teleoperated by EMG signals and arm motions,” *IEEE Trans. Robot. Autom.*, 2003, doi: 10.1109/TRA.2003.808873.

[12] P. K. Artemiadis and K. J. Kyriakopoulos, “A switching regime model for the emg-based control of a robot arm,” *IEEE Trans. Syst. Man, Cybern. Part B Cybern.*, vol. 41, no. 1, pp. 53–63, 2011, doi: 10.1109/TSMCB.2010.2045120.

[13] P. K. Artemiadis and K. J. Kyriakopoulos, “EMG-based control of a robot arm using low-dimensional embeddings,” *IEEE Trans. Robot.*, vol. 26, no. 2, pp. 393–398, 2010, doi: 10.1109/TRO.2009.2039378.

[14] S. I. Benchabane, N. Saadia, and A. Ramdane-Cherif, “Novel algorithm for

conventional myocontrol of upper limbs prosthetics," *Biomed. Signal Process. Control*, vol. 57, p. 101791, 2020, doi: 10.1016/j.bspc.2019.101791.

[15] H. J. Liu and K. Y. Young, "An adaptive upper-arm EMG-based robot control system," *Int. J. Fuzzy Syst.*, vol. 12, no. 3, pp. 181–189, 2010.

[16] J. J. A. M. Junior, M. B. Pires, S. Okida, and S. L. Stevan, "Robotic Arm Activation using Surface Electromyography with LABVIEW," *IEEE Lat. Am. Trans.*, vol. 14, no. 8, pp. 3597–3605, 2016, doi: 10.1109/TLA.2016.7786339.

[17] I. Vujaklija, D. Farina, and O. C. Aszmann, "New developments in prosthetic arm systems," *Orthop. Res. Rev.*, vol. 8, pp. 31–39, 2016, doi: 10.2147/ORR.S71468.

[18] A. Krasoulis and K. Nazarpour, "Myoelectric digit action decoding with multi-label, multi-class classification: an offline analysis," *Sci. Rep.*, pp. 1–10, 2020, doi: 10.1101/2020.03.24.005710.

[19] S. Sharma and A. K. Dubey, "Movement control of robot in real time using EMG signal," *ICPCES 2012 - 2012 2nd Int. Conf. Power, Control Embed. Syst.*, 2012, doi: 10.1109/ICPCES.2012.6508060.

[20] J. L. Pons, *Wearable Robots: Biomechatronic Exoskeletons*. John Wiley & Sons, 2008.

[21] G. Jang, J. Kim, Y. Choi, and J. Yim, "Human shoulder motion extraction using EMG signals," *Int. J. Precis. Eng. Manuf.*, vol. 15, no. 10, pp. 2185–2192, 2014, doi: 10.1007/s12541-014-0580-x.

[22] L. J. Hargrove, K. Englehart, and B. Hudgins, "A comparison of surface and intramuscular myoelectric signal classification," *IEEE Trans. Biomed. Eng.*, vol. 54, no. 5, pp. 847–853, 2007, doi: 10.1109/TBME.2006.889192.

[23] A. Jaramillo-Yánez, M. E. Benalcázar, and E. Mena-Maldonado, "Real-time hand

gesture recognition using surface electromyography and machine learning: A systematic literature review," *Sensors (Switzerland)*, vol. 20, no. 9, pp. 1–36, 2020, doi: 10.3390/s20092467.

[24] N. Parajuli *et al.*, "Real-time EMG based pattern recognition control for hand prostheses: A review on existing methods, challenges and future implementation," *Sensors (Switzerland)*, vol. 19, no. 20, 2019, doi: 10.3390/s19204596.

[25] R. C. Gopura, S. V. Bandara, and M. P. Gunasekara, "Recent Trends in EMG-Based Control Methods for Assistive Robots," in *Electrodiagnosis in New Frontiers of Clinical Research*, IntechOpen, 2013, pp. 237–268.

[26] M. Simao, N. Mendes, O. Gibaru, and P. Neto, "A Review on Electromyography Decoding and Pattern Recognition for Human-Machine Interaction," *IEEE Access*, vol. 7, no. c, pp. 39564–39582, 2019, doi: 10.1109/ACCESS.2019.2906584.

[27] A. J. Young, L. H. Smith, E. J. Rouse, and L. J. Hargrove, "A comparison of the real-time controllability of pattern recognition to conventional myoelectric control for discrete and simultaneous movements," *J. Neuroeng. Rehabil.*, vol. 11, no. 1, pp. 1–10, 2014, doi: 10.1186/1743-0003-11-5.

[28] H. F. Hassan, S. J. Abou-Loukh, and I. K. Ibraheem, "Teleoperated robotic arm movement using electromyography signal with wearable Myo armband," *J. King Saud Univ. - Eng. Sci.*, no. xxxx, 2019, doi: 10.1016/j.jksues.2019.05.001.

[29] A. Phinyomark, R. N. Khushaba, and E. Scheme, "Feature extraction and selection for myoelectric control based on wearable EMG sensors," *Sensors (Switzerland)*, vol. 18, no. 5, May 2018, doi: 10.3390/s18051615.

[30] A. Phinyomark, P. Phukpattaranont, and C. Limsakul, "Feature reduction and selection for EMG signal classification," *Expert Syst. Appl.*, vol. 39, no. 8, pp.

7420–7431, 2012, doi: 10.1016/j.eswa.2012.01.102.

[31] A. Phinyomark, S. Hirunviriya, C. Limsakul, and P. Phukpattaranont, “Evaluation of EMG feature extraction for hand movement recognition based on euclidean distance and standard deviation,” *ECTI-CON 2010 - 2010 ECTI Int. Conf. Electr. Eng. Comput. Telecommun. Inf. Technol.*, no. May 2016, pp. 856–860, 2010.

[32] M. Paluszek and S. Thomas, *MATLAB Machine Learning*. 2019.

[33] C. Cortes and V. Vladimir, “Support-Vector Networks,” *Mach. Leaming*, vol. 20, no. 3, pp. 273–297, 1995, doi: 10.1109/64.163674.

[34] T. G. Dietterich, “Ensemble methods in machine learning,” *Lect. Notes Comput. Sci. (including Subser. Lect. Notes Artif. Intell. Lect. Notes Bioinformatics)*, vol. 1857 LNCS, pp. 1–15, 2000, doi: 10.1007/3-540-45014-9_1.

[35] S. Duprey, A. Naaim, F. Moissenet, M. Begon, and L. Chèze, “Kinematic models of the upper limb joints for multibody kinematics optimisation: An overview,” *J. Biomech.*, vol. 62, pp. 87–94, 2017, doi: 10.1016/j.jbiomech.2016.12.005.

[36] A. Campeau-Lecours, U. Cote-Allard, D. S. Vu, F. Routhier, B. Gosselin, and C. Gosselin, “Intuitive Adaptive Orientation Control for Enhanced Human-Robot Interaction,” *IEEE Trans. Robot.*, vol. 35, no. 2, pp. 509–520, 2019, doi: 10.1109/TRO.2018.2885464.

[37] P. K. Artemiadis and K. J. Kyriakopoulos, “An EMG-based robot control scheme robust to time-varying EMG signal features,” *IEEE Trans. Inf. Technol. Biomed.*, vol. 14, no. 3, pp. 582–588, 2010, doi: 10.1109/TITB.2010.2040832.

[38] T. Tsuji, T. Shibanoki, and K. Shima, “EMG-Based Control of a Multi-Joint Robot for Operating a Glovebox,” *Handb. Res. Adv. Robot. Mechatronics*, pp. 36–52, 2015, doi: 10.4018/978-1-4666-7387-8.ch003.

[39] S. Shin, R. Tafreshi, and R. Langari, “EMG and IMU based real-time HCI using dynamic hand gestures for a multiple-DoF robot arm,” *J. Intell. Fuzzy Syst.*, vol. 35, no. 1, pp. 861–876, 2018, doi: 10.3233/JIFS-171562.

[40] P. W. Laksono, M. Sasaki, K. Matsushita, M. S. A. bin Suhaimi, and J. Muguro, “Preliminary Research of Surface Electromyogram (sEMG) Signal Analysis for Robotic Arm Control,” in *The 5th International Conference on Industrial, Mechanical, Electrical, and Chemical Engineering 2019 (ICIMECE 2019)*, 2019, p. 6.

[41] V. Villani, F. Pini, F. Leali, and C. Secchi, “Survey on human–robot collaboration in industrial settings: Safety, intuitive interfaces and applications,” *Mechatronics*, vol. 55, no. February, pp. 248–266, 2018, doi: 10.1016/j.mechatronics.2018.02.009.

[42] S. Benatti, B. Milosevic, E. Farella, E. Gruppioni, and L. Benini, “A Prosthetic Hand Body Area Controller Based on Efficient Pattern Recognition Control Strategies,” *Sensors*, vol. 17, no. 4, p. 869, 2017, doi: 10.3390/s17040869.

[43] N. Nazmi, M. A. A. Rahman, S. I. Yamamoto, S. A. Ahmad, H. Zamzuri, and S. A. Mazlan, “A review of classification techniques of EMG signals during isotonic and isometric contractions,” *Sensors (Switzerland)*, vol. 16, no. 8, pp. 1–28, 2016, doi: 10.3390/s16081304.

[44] G. Rasoo, K. Iqbal, N. Bouaynaya, and G. White, “Real-time task discrimination for myoelectric control employing task-specific muscle synergies,” *IEEE Trans. Neural Syst. Rehabil. Eng.*, vol. 24, no. 1, pp. 98–108, 2016, doi: 10.1109/TNSRE.2015.2410176.

[45] Triwiyanto, T. Rahmawati, E. Yulianto, M. R. Mak’ruf, and P. C. Nugraha,

"Dynamic feature for an effective elbow-joint angle estimation based on electromyography signals," *Indones. J. Electr. Eng. Comput. Sci.*, vol. 19, no. 1, pp. 178–187, 2020, doi: 10.11591/ijeecs.v19.i1.pp178-187.

[46] O. W. Samuel and M. G. Asogbon, "Intelligent EMG Pattern Recognition Control Method for Upper-Limb Multifunctional Prostheses : Advances , Current Challenges , and Future Prospects," *IEEE Access*, vol. PP, no. c, p. 1, 2019, doi: 10.1109/ACCESS.2019.2891350.

[47] D. Farina *et al.*, "The extraction of neural information from the surface EMG for the control of upper-limb prostheses: Emerging avenues and challenges," *IEEE Trans. Neural Syst. Rehabil. Eng.*, vol. 22, no. 4, pp. 797–809, 2014, doi: 10.1109/TNSRE.2014.2305111.

[48] D. C. Toledo-Pérez, J. Rodríguez-Reséndiz, R. A. Gómez-Loenzo, and J. C. Jauregui-Correa, "Support Vector Machine-based EMG signal classification techniques: A review," *Appl. Sci.*, vol. 9, no. 20, 2019, doi: 10.3390/app9204402.

[49] G. Jia, H. K. Lam, J. Liao, and R. Wang, "Classification of electromyographic hand gesture signals using machine learning techniques," *Neurocomputing*, vol. 401, pp. 236–248, 2020, doi: 10.1016/j.neucom.2020.03.009.

[50] M. I. Rusydi, M. Sasaki, and S. Ito, "Affine transform to reform pixel coordinates of EOG signals for controlling robot manipulators using gaze motions," *Sensors (Switzerland)*, vol. 14, no. 6, pp. 10107–10123, 2014, doi: 10.3390/s140610107.

[51] J. R. García-Sánchez *et al.*, "Robust switched tracking control for wheeled mobile robots considering the actuators and drivers," *Sensors (Switzerland)*, vol. 18, no. 12, pp. 1–21, 2018, doi: 10.3390/s18124316.

[52] N. Wang, K. Lao, and X. Zhang, "Design and Myoelectric Control of an

Anthropomorphic Prosthetic Hand," *J. Bionic Eng.*, vol. 14, no. 1, pp. 47–59, 2017, doi: 10.1016/S1672-6529(16)60377-3.

[53] J. De Jesús Rubio *et al.*, "Structure regulator for the perturbations attenuation in a quadrotor," *IEEE Access*, vol. 7, no. May 2020, pp. 138244–138252, 2019, doi: 10.1109/ACCESS.2019.2941232.

[54] M. Tavakoli, C. Benussi, and J. L. Lourenco, "Single channel surface EMG control of advanced prosthetic hands: A simple, low cost and efficient approach," *Expert Syst. Appl.*, vol. 79, pp. 322–332, 2017, doi: https://doi.org/10.1016/j.eswa.2017.03.012.

[55] C. W. Antuvan, M. Ison, and P. Artemiadis, "Embedded human control of robots using myoelectric interfaces," *IEEE Trans. Neural Syst. Rehabil. Eng.*, vol. 22, no. 4, pp. 820–827, 2014, doi: 10.1109/TNSRE.2014.2302212.

[56] D. I. Martinez *et al.*, "Stabilization of Robots with a Regulator Containing the Sigmoid Mapping," *IEEE Access*, vol. 8, no. May, pp. 89479–89488, 2020, doi: 10.1109/ACCESS.2020.2994004.

[57] M. S. A. Bin Suhaimi, K. Matsushita, M. Sasaki, and W. Njeri, "24-Gaze-Point Calibration Method for Improving the Precision of Ac-Eog Gaze Estimation," *Sensors (Switzerland)*, vol. 19, no. 17, 2019, doi: 10.3390/s19173650.

[58] L. E. Sánchez-Velasco, M. Arias-Montiel, E. Guzmán-Ramírez, and E. Lugo-González, "A Low-Cost EMG-Controlled Anthropomorphic Robotic Hand for Power and Precision Grasp," *Biocybern. Biomed. Eng.*, vol. 40, no. 1, pp. 221–237, 2020, doi: https://doi.org/10.1016/j.bbe.2019.10.002.

[59] C. Aguilar-Ibanez and M. S. Suarez-Castanon, "A Trajectory Planning Based Controller to Regulate an Uncertain 3D Overhead Crane System," *Int. J. Appl.*

Math. Comput. Sci., vol. 29, no. 4, pp. 693–702, 2020, doi: 10.2478/amcs-2019-0051.

[60] C. Fang, B. He, Y. Wang, J. Cao, and S. Gao, "EMG-Centered Multisensory Based Technologies for Pattern Recognition in Rehabilitation : State of the Art and Challenges," *Biosensors*, vol. 10, no. 85, pp. 1–30, 2020, doi: 10.3390/bios10080085.

[61] U. Qidwai, M. S. Ajimsha, and M. Shakir, "The role of EEG and EMG combined virtual reality gaming system in facial palsy rehabilitation - A case report," *J. Bodyw. Mov. Ther.*, vol. 23, no. 2, pp. 425–431, 2019, doi: https://doi.org/10.1016/j.jbmt.2019.02.012.

[62] A. Chowdhury, H. Raza, Y. K. Meena, A. Dutta, and G. Prasad, "An EEG-EMG correlation-based brain-computer interface for hand orthosis supported neuro-rehabilitation," *J. Neurosci. Methods*, vol. 312, pp. 1–11, 2019, doi: https://doi.org/10.1016/j.jneumeth.2018.11.010.

[63] D. Ramírez-Martínez, M. Alfaro-Ponce, O. Pogrebnyak, M. Aldape-Pérez, and A.-J. Argüelles-Cruz, "Hand Movement Classification Using Burg Reflection Coefficient," *Sensors*, vol. 19, no. 475, pp. 1–18, 2019, doi: 10.3390/s19030475.

[64] S. M. M. Rahman, "Machine Learning-Based Cognitive Position and Force Controls for Power-Assisted Human – Robot Collaborative Manipulation," *Machines*, 2021.

[65] S. Zhou, K. Yin, F. Fei, and K. Zhang, "Surface electromyography–based hand movement recognition using the Gaussian mixture model, multilayer perceptron, and AdaBoost method," *Int. J. Distrib. Sens. Networks*, vol. 15, no. 4, 2019, doi: 10.1177/1550147719846060.

[66] R. N. Khushaba, S. Kodagoda, M. Takruri, and G. Dissanayake, “Expert Systems with Applications Toward improved control of prosthetic fingers using surface electromyogram (EMG) signals,” *Expert Syst. Appl.*, vol. 39, no. 12, pp. 10731–10738, 2012, doi: 10.1016/j.eswa.2012.02.192.

[67] A. K. Mukhopadhyay and S. Samui, “An experimental study on upper limb position invariant EMG signal classification based on deep neural network,” *Biomed. Signal Process. Control*, vol. 55, p. 101669, 2020, doi: 10.1016/j.bspc.2019.101669.

[68] A. J. Ko, T. D. LaToza, and M. M. Burnett, “A practical guide to controlled experiments of software engineering tools with human participants,” *Empir. Softw. Eng.*, vol. 20, no. 1, pp. 110–141, 2013, doi: 10.1007/s10664-013-9279-3.

[69] M. Faber, J. Bützler, and C. M. Schlick, “Human-robot Cooperation in Future Production Systems: Analysis of Requirements for Designing an Ergonomic Work System,” *Procedia Manuf.*, vol. 3, no. Ahfe, pp. 510–517, 2015, doi: 10.1016/j.promfg.2015.07.215.

[70] Y. Huang, K. Chen, X. Zhang, K. Wang, and J. Ota, “Joint torque estimation for the human arm from sEMG using backpropagation neural networks and autoencoders,” *Biomed. Signal Process. Control*, vol. 62, p. 102051, 2020, doi: 10.1016/j.bspc.2020.102051.

[71] S. Márquez-figueroa, Y. S. Shmaliy, and O. Ibarra-manzano, “Biomedical Signal Processing and Control Optimal extraction of EMG signal envelope and artifacts removal assuming colored measurement noise,” *Biomed. Signal Process. Control*, vol. 57, p. 101679, 2020, doi: 10.1016/j.bspc.2019.101679.

[72] K. Englehart and B. Hudgins, “A Robust, Real-Time Control Scheme for

Multifunction Myoelectric Control," *IEEE Trans. Biomed. Eng.*, vol. 50, no. 7, pp. 848–854, 2003, doi: 10.1109/TBME.2003.813539.

[73] O. W. Samuel *et al.*, "Intelligent EMG pattern recognition control method for upper-limb multifunctional prostheses: Advances, current challenges, and future prospects," *IEEE Access*, vol. 7, pp. 10150–10165, 2019, doi: 10.1109/ACCESS.2019.2891350.

[74] C. W. Antuvan, F. Bisio, F. Marini, S. C. Yen, E. Cambria, and L. Masia, "Role of Muscle Synergies in Real-Time Classification of Upper Limb Motions using Extreme Learning Machines," *J. Neuroeng. Rehabil.*, vol. 13, no. 1, pp. 1–15, 2016, doi: 10.1186/s12984-016-0183-0.

[75] F. Nougarou, A. Campeau-lecours, D. Massicotte, M. Boukadoum, and C. Gosselin, "Biomedical Signal Processing and Control Pattern recognition based on HD-sEMG spatial features extraction for an efficient proportional control of a robotic arm," *Biomed. Signal Process. Control*, vol. 53, p. 101550, 2019, doi: 10.1016/j.bspc.2019.04.027.

[76] N. Rabin, M. Kahlon, S. Malayev, and A. Ratnovsky, "Classification of human hand movements based on EMG signals using nonlinear dimensionality reduction and data fusion techniques," *Expert Syst. Appl.*, vol. 149, p. 113281, 2020, doi: 10.1016/j.eswa.2020.113281.

[77] A. J. Young, L. H. Smith, E. J. Rouse, and L. J. Hargrove, "A comparison of the real-time controllability of pattern recognition to conventional myoelectric control for discrete and simultaneous movements," *J. Neuroeng. Rehabil.*, vol. 11, no. 1, pp. 1–10, 2014, doi: 10.1186/1743-0003-11-5.

[78] Y. Jiang *et al.*, "Shoulder muscle activation pattern recognition based on sEMG

and machine learning algorithms," *Comput. Methods Programs Biomed.*, vol. 197, 2020, doi: 10.1016/j.cmpb.2020.105721.

[79] A. Tsai, T. Hsieh, J. Luh, and T. Lin, "A comparison of upper-limb motion pattern recognition using EMG signals during dynamic and isometric muscle contractions," *Biomed. Signal Process. Control*, vol. 11, pp. 17–26, 2014, doi: 10.1016/j.bspc.2014.02.005.

[80] E. Trigili *et al.*, "Detection of movement onset using EMG signals for upper-limb exoskeletons in reaching tasks," *J. Neuroeng. Rehabil.*, vol. 16, no. 1, pp. 1–16, 2019.

[81] X. Li, P. Zhou, and A. S. Aruin, "Teager–Kaiser Energy Operation of Surface EMG Improves Muscle Activity Onset Detection," *Ann. Biomed. Eng.*, vol. 35, no. 9, pp. 1532–1538, 2007, doi: 10.1007/s10439-007-9320-z.

[82] J. F. Kaiser, "Some useful properties of Teager's energy operators," in *Proceedings - ICASSP, IEEE International Conference on Acoustics, Speech and Signal Processing*, 1993, vol. 3, pp. 111.149-152, [Online]. Available: https://www.scopus.com/inward/record.uri?eid=2-s2.0-0027210171&partnerID=40&md5=4a9c0b31b734581894f9f5a3c234988b.

[83] R. H. Chowdhury, M. B. I. Reaz, M. A. Bin Mohd Ali, A. A. A. Bakar, K. Chellappan, and T. G. Chang, "Surface electromyography signal processing and classification techniques," *Sensors*, vol. 13, no. 9, pp. 12431–12466, 2013, doi: 10.3390/s130912431.

[84] D. Karabulut, F. Ortes, Y. Z. Arslan, and M. A. Adli, "Comparative evaluation of EMG signal features for myoelectric controlled human arm prosthetics," *Biocybern. Biomed. Eng.*, vol. 37, no. 2, pp. 326–335, 2017, doi:

10.1016/j.bbe.2017.03.001.

[85] A. Phinyomark, P. Phukpattaranont, and C. Limsakul, “Feature reduction and selection for EMG signal classification,” *Expert Syst. Appl.*, 2012, doi: 10.1016/j.eswa.2012.01.102.

[86] L. Rokach, A. Schclar, and E. Itach, “Ensemble methods for multi-label classification,” *Expert Syst. Appl.*, vol. 41, no. 16, pp. 7507–7523, 2014, doi: 10.1016/j.eswa.2014.06.015.

[87] A. Noor, M. K. Ucąr, K. Polat, A. Assiri, R. Nour, and E. Masciari, “A Novel Approach to Ensemble Classifiers: FsBoost-Based Subspace Method,” *Math. Probl. Eng.*, vol. 2020, 2020, doi: 10.1155/2020/8571712.

[88] L. H. Smith, L. J. Hargrove, B. A. Lock, and T. A. Kuiken, “Classification Error and Controller Delay,” *IEEE Trans. Neural Syst. Rehabil. Eng.*, vol. 19, no. 2, pp. 186–192, 2011, doi: 10.1109/TNSRE.2010.2100828.Determining.

RELATED PUBLICATIONS

Journal Articles

1. **Laksono, Pringgo Widyo**.; Matsushita, Kojiro.; Suhaimi, Muhammad Syaiful Amri bin.; Kitamura, Takahide; Njeri, Waweru; Muguro, Josheph.; Sasaki, Minoru. **Mapping Three Electromyography Signals Generated by Human Elbow and Shoulder Movements to Two Degree of Freedom Upper-Limb Robot Control**. *Robotics* **2020**, *9*, 83. https://doi.org/10.3390/robotics9040083 (Scopus & WOS)
2. **Laksono, Pringgo Widyo**.; Kitamura, Takahide; Muguro, Josheph; Matsushita, Kojiro; Sasaki, Minoru; Suhaimi, Muhammad Syaiful Amri bin**. Minimum Mapping from EMG Signals at Human Elbow and Shoulder Movements into Two DoF Upper-Limb Robot with Machine Learning.** *Machines* **2021**, 9, 56. https://doi.org/10.3390/machines9030056 (Scopus & WOS)
3. Sasaki, M.; Matsushita, K.; Rusyidi, M. I.; **Laksono, P. W**.; Muguro, J.; Syaiful, M.; Njeri, W.; Sasaki, M.; Matsushita, K.; Rusyidi, M. I.; Laksono, P. W. **Estimation of The Shoulder Joint Angle Using Brainwaves**, Andalas Journal of Electrical and Electronic Engineering Technology (AJEEET), 2021, 1,1,1-14.

Proceeding Articles

1. Sasaki, M.; Matsushita, K.; Rusyidi, M. I.; **Laksono, P. W**.; Muguro, J.; Syaiful, M.; Njeri, W.; Sasaki, M.; Matsushita, K.; Rusyidi, M. I.; Laksono, P. W. Robot Control Systems Using Bio-Potential Signals Robot Control Systems Using Bio-Potential Signals. In The 5th International Conference on Industrial, Mechanical Electrical, and Chemical Engineering 2019 (ICIMECE 2019); AIP Conference Proceedings 2217, 020008 (2020); https://doi.org/10.1063/5.0000624

2. Muguro, J. K.; Sasaki, M.; Matsushita, K.; Njeri, W.; **Laksono, P. W**.; Muguro, J. K.; Sasaki, M.; Matsushita, K. Development of Neck Surface Electromyography Gaming Control Interface for Application in Tetraplegic Patients ' Entertainment Development of Neck Surface Electromyography Gaming Control Interface for Application in Tetraplegic Patients' Entertainment. In The 5th International Conference on Industrial, Mechanical Electrical, and Chemical Engineering 2019 (ICIMECE 2019) AIP Conference Proceedings 2217,030039(2020; https://doi.org/10.1063/5.0000500
3. **Laksono, P. W**.; Sasaki, M.; Matsushita, K.; Suhaimi, M. S. A. bin; Muguro, J. Preliminary Research of Surface Electromyogram (SEMG) Signal Analysis for Robotic Arm Control. In The 5th International Conference on Industrial, Mechanical, Electrical, and Chemical Engineering 2019 (ICIMECE 2019); AIP Conference Proceedings 2217, 030034 (2020); https://doi.org/10.1063/5.0000542